

Lawrence Berkeley National Laboratory

Recent Work

Title

GLIDE AND CLIMB OF PRISMATIC DISLOCATION HALF-LOOPS IN HIGHLY PERFECT COPPER CRYSTALS

Permalink

<https://escholarship.org/uc/item/40h9k3s6>

Author

Miura, Yasuhiro.

Publication Date

1970-08-01

LAWRENCE
RADIATION LABORATORY

UCRL-19625

c 2

OCT 23 1970

LIBRARY AND
DOCUMENTS SECTION

GLIDE AND CLIMB OF PRISMATIC DISLOCATION
HALF-LOOPS IN HIGHLY PERFECT COPPER CRYSTALS

Yasuhiro Miura
(Ph. D. Thesis)

August 1970

AEC Contract No. W-7405-eng-48

TWO-WEEK LOAN COPY

*This is a Library Circulating Copy
which may be borrowed for two weeks.
For a personal retention copy, call
Tech. Info. Division, Ext. 5545*

LAWRENCE RADIATION LABORATORY
UNIVERSITY of CALIFORNIA BERKELEY

UCRL-19625

DISCLAIMER

This document was prepared as an account of work sponsored by the United States Government. While this document is believed to contain correct information, neither the United States Government nor any agency thereof, nor the Regents of the University of California, nor any of their employees, makes any warranty, express or implied, or assumes any legal responsibility for the accuracy, completeness, or usefulness of any information, apparatus, product, or process disclosed, or represents that its use would not infringe privately owned rights. Reference herein to any specific commercial product, process, or service by its trade name, trademark, manufacturer, or otherwise, does not necessarily constitute or imply its endorsement, recommendation, or favoring by the United States Government or any agency thereof, or the Regents of the University of California. The views and opinions of authors expressed herein do not necessarily state or reflect those of the United States Government or any agency thereof or the Regents of the University of California.

TABLE OF CONTENTS

ABSTRACT

I. INTRODUCTION----- 1

II. EXPERIMENTAL PROCEDURES----- 5

 A. Material----- 5

 B. Growth of Low Dislocation Density Crystals----- 5

 C. Thermal Cyclic Annealing----- 6

 D. Techniques of Direct Observation of Dislocation----- 7

 E. Punching of Prismatic Dislocation Half-Loops----- 10

 F. Shape of Half-Loops----- 11

 G. Glide of Half-Loops----- 11

 H. Climb of Half-Loops----- 13

III. RESULTS----- 14

 A. Effects of Thermal Cyclic Annealing----- 14

 B. Prismatic Dislocation Half-Loops----- 14

 C. Geometry of Etch Pits----- 15

 D. Shape of Half Loops----- 15

 E. Glide of Prismatic Dislocation Half-Loops-----16

 F. Climb of Prismatic Dislocation Half-Loops----- 17

IV. DISCUSSIONS----- 19

 A. Shape of Half-Loops----- 19

 B. Glide of Half-Loops----- 20

 C. Minimum Energy Configuration of Half-Loops----- 25

 D. Twist of Half-Loops in Glide Cylinder ----- 26

 E. Climb of Half-Loops----- 27

V. CONCLUSIONS-----	33
A. Shape of Half-Loops and Glide-----	33
B. Climb-----	34
VI. APPENDIX: Sample of Calculation of the Critical Shear Stress to Move a Loop Using Bullough and Newmans Equations-----	35
ACKNOWLEDGEMENTS-----	37
REFERENCES-----	38
FIGURE CAPTIONS-----	40
FIGURES-----	44

GLIDE AND CLIMB OF PRISMATIC DISLOCATION HALF-LOOPS IN
HIGHLY PERFECT COPPER CRYSTALS

Yasuhiro Miura

Inorganic Materials Research Division, Lawrence Radiation Laboratory
Department of Materials Science and Engineering, College of Engineering
University of California, Berkeley, California

ABSTRACT

Glide and climb of punched out prismatic edge dislocation half-loops in copper crystals were studied by a dislocation etch pit technique. Improved crystal growing procedures yielded copper crystals of dislocation density less than 10^3 cm/cm³ so that rows of large prismatic dislocation half-loops (radius $\approx 10\mu$) with Burgess vectors $\langle 110 \rangle$ could be introduced by a ball indentation on a $\{111\}$ plane in an originally dislocation-free area of the crystal. Both a dislocation etch pit picture and an X-ray transmission topograph proved the low dislocation density of the crystals.

The half-loops were microscopically approximately semicircular in shape. For dislocation glide it was found that larger loops were more highly mobile than smaller ones. This was attributed to a lower dislocation step density of large loops.

Corners of steps were assumed to be rounded; that is, the dislocation line at corners of steps lies on planes other than $\{111\}$. A higher lattice frictional stress acts to oppose motion of a dislocation on non-close packed planes. Therefore, the corners of steps may act as pinning points on gliding dislocation half-loops. It was also found that, within a single half-loop, the segment with higher step density was less mobile.

When half-loops were annealed at a temperature where diffusion is

rapid, they shrank. Macroscopically loops maintained approximately a semicircular shape during the process of shrinkage. The shrinkage curve $r^2 - t$ was approximately linear (r is the radius of loop and t is the annealing time) and the apparent activation energy of shrinkage was ≈ 1.28 eV. The results were best interpreted by a model based on vacancy formation at the point of intersection of the dislocation and the crystal surface and pipe diffusion along the dislocation loop.

I. INTRODUCTION

Glide and climb of a single dislocation are the elementary processes of the mechanical behavior of crystalline solids. It is essential to have a well characterized dislocation for the object of study. In the present work, the motion of indentation punched prismatic edge dislocation half-loops in copper crystals will be studied, first the glide at very small stresses and secondly the climb by diffusion of point defects.

1. Glide

Resistance to conservative motion of dislocation in face centered cubic metals has been studied by many investigators using a wide variety of techniques. Particularly pertinent to the present work are the experiments of Young.¹⁻⁸ He found that some dislocations started moving at a resolved shear stress of 4 g/mm^2 , dislocation multiplication took place at $15\text{-}20 \text{ g/mm}^2$ and macroscopic yielding occurred at the stress of 35 g/mm^2 .

The percentage of growth in dislocations moved by the applied stress increased monotonically with the stress until approximately 75% had been moved at the yield stress. Fresh dislocations were observed to move at lower stresses than grown-in dislocations. The latter could have been pinned by impurity atoms. He concluded that impurity pinning does greatly affect the motion of dislocations even in highly pure crystals (nominally 99.999% Cu).

According to Marukawa,⁹ dislocation velocity in low dislocation density copper crystals is much larger than in LiF ³⁰ or silicon iron³¹ and the distance moved by a dislocation varies little with the loading time. This suggests that dislocations are held up at widely spaced

barriers.

Petroff and Washburn¹⁰ measured the stresses at which individual segments of grown in dislocations began to move, obtaining results similar to Young's. They attributed the range of critical stresses for motion to different jog densities depending on the different dislocation lines. This interpretation was supported by the fact that the critical shear stress for motion of a heavily jogged prismatic edge dislocation half-loop was found to be greater than 50 g/mm^2 .

The observations above were all carried out at room temperature using the dislocation etch pit technique to record dislocation movement.

The main difficulties for an etch pit study on copper are: first, the obtaining of specimens of a low enough dislocation density, secondly a single etch pit picture can give no information on the internal dislocation arrangement. Yet the technique is powerful when applied to bulk crystals.

Previous workers, except Petroff and Washburn, did not pay much attention to the internal configuration of dislocation lines. More precise information on dislocation motion in copper crystals can be obtained only by careful studies on well characterized dislocations.

In the present work, the origins of frictional stress are studied on dislocations of a particular shape; prismatic edge dislocation half loops of various sizes which are introduced by a ball indentation in extremely low dislocation density crystals.

The critical shear stress for motion of indentation punched prismatic dislocation half-loops of different sizes are estimated using the theoretical equations of Bullough and Newman.¹¹

The twist motion of a half-loop on the glide cylinder under the operation of bending stresses is also studied in order to see the difference in mobility between the different dislocation segments within a single half-loop.

2. Climb

Dislocation motion perpendicular to the glide plane requires the production or absorption of point defects and so occurs only above a temperature about one half of the melting point of the metal or at stresses approaching the theoretical strength.

Silcox and Whelan,¹² using a hot stage transmission electron microscopy were first to directly observe the shrinkage of dislocation loops by climb. Prismatic dislocation loops in face-centered cubic metals are expected to shrink at observable rates at temperatures where diffusion becomes appreciable.

The climb mechanism has been considered theoretically by Friedel.¹³ His theory of dislocation climb is based on vacancy diffusion away from jog sites which move along the dislocation line.

Silcox and Whelan's measurements of the shrinkage rates of prismatic dislocation loops in aluminum thin foils were interpreted in terms of Friedel's theory. When line tension is the only driving force for climb, the loop diameter should decrease with annealing time according to a parabolic relation. Silcox and Whelan's experimental observations were in general agreement with this prediction. The activation energy of self diffusion has been estimated by comparing the shrinkage rates of loops of the same size at different annealing temperatures.

The climb model of Silcox and Whelan has been universally employed by many workers to interpret their experimental results.

However, since exact shape of dislocation loops, the jog density and the dislocation core structures are not known, any model of climb contains assumptions.

Seidman and Balluffi¹⁴ discussed the climb mechanism for aluminum and suggested that vacancy diffusion away from the dislocation should often be the rate-controlling process rather than the vacancy-emission rate as was assumed by Friedel. Their analysis is based on an assumption that a vacancy dislocation loop is a perfect torus shaped source of vacancies.

In the present works, the primary purpose is to know whether the shrinkage of indentation punched dislocation half-loops in copper is best explained by an emission or a diffusion controlled mechanism.

For an indentation punched surface half-loop, a smaller apparent activation energy for shrinkage might be expected, because vacancies can be supplied from the external surface through an easy diffusion pipe along the dislocation line itself as well as by bulk diffusion.

In the present work, shrinkage rates of half-loops at different temperatures are obtained and the apparent activation energy of shrinkage is deduced. The shrinkage mechanism is discussed.

II. EXPERIMENTAL PROCEDURES

A. Material

Copper rods of 19 mm diameter with a purity of 99.999% Cu were obtained from Materials Research Corporation. Results of spectrographic analysis were as follows; (numbers are in ppm)

Fe	Ni	Si	Sb	Pb	Sn	Bi	Ag	As	Cr	Te	Se*	S*
<0.7	< 1	<0.1	< 1	< 1	< 1	<0.1	<0.3	< 2	<0.5	< 2	< 1	< 1

* Chemical analysis. Other elements not detected.

B. Growth of Low Dislocation Density Crystals

One of the main requirements of the present work was to obtain specimens with an extremely low dislocation density, preferably less than 10^3 cm/cm³. Much time was spent on the development of a successful crystal-growing technique. The procedures which were finally established are schematically shown in Fig. 1. First spherical single crystals of 25 mm diameter were grown by the Bridgmann technique (furnace traveling speed was five centimeter per hour), then cylindrical crystals of 10 mm diameter were grown with a $\langle 111 \rangle$ growth direction using the spherical crystals as seeds (furnace traveling speed was 5 cm per hour). Finally, larger cylindrical crystals, 32 mm diameter, were grown using the 10 mm diameter crystals as seeds. A zig-zag shape near the seed was used to avoid any direct influence of the dislocation substructure in the seed on the dislocation arrangement in the grown crystal. Dislocation lines are expected to propagate perpendicularly to the moving liquid-solid interface in order to minimize the line energy.

All melting was carried out under vacuum. The 32 mm diameter crystals were placed on a goniometer and oriented to be cut by an acid saw into 5 mm thick discs with face-parallel to (111) planes. Thinner discs were cut out for anomalous transmission x-ray topographs. Discs were polished on an acid lathe and finally cut into parallelepipeds on the acid saw. The geometry of the parallelepipeds is shown in Fig. 3. The polishing solution for the acid lathe consisted of two parts HNO_3 , one part H_3PO_4 and one part CH_3COOH glacial. Concentrated nitric acid was used for acid saw cutting. Finally the parallelepiped crystals were electropolished at room temperature in a 50% phosphoric acid-40% water solution.

The dislocation density was revealed by the etch pit technique on the (111) faces. Dislocation density of as grown crystals was $1 \sim 5 \times 10^5 \text{ cm/cm}^3$.

C. Thermal Cyclic Annealing

For the further reduction of the dislocation density, specimens were annealed at a temperature just below the melting point. By annealing at constant temperature (1070°C) for a week the dislocation density was reduced from 5×10^5 to $1 \times 10^5 \text{ cm/cm}^3$ and many subgrain boundaries were formed.

Thermal cyclic annealing was then employed because of these rather discouraging results from static annealing. There are two convenient ways periodically to change the temperature. Livingston,¹⁵ Young,¹⁶ and other workers have cycled the temperature by switching the furnace current on and off. They reported on appreciable effects due to cyclic annealing on the rate of change of dislocation density.

Kitajima et al.¹⁷ reported excellent results from cyclic annealing by translating the furnace back and forth, while keeping the furnace tube and specimens stationary. They obtained a reduction of dislocation density

down to the order of 10^3 cm/cm³ in as grown crystals which contained $10^5 \sim 10^6$ cm/cm³. They explained that the rapid reduction of the dislocations was possibly due to the enhanced flow of point defects by the temperature gradients within a crystal.

An annealing furnace (Fig. 3) was designed similar to the one used by Kitajima et al. A helium gas atmosphere was chosen because it was available with negligible oxygen and water vapor impurity.

A temperature-time chart for a typical specimen is shown in Fig. 4. Maximum and minimum temperature were approximately 1050°C and 800°C respectively. The furnace traveled back and forth at a speed of 100 cm per hour. Also the system was designed in such a way that the length of furnace travel could be adjusted between 0 and 25 cm on each side of the center and the furnace traveling speed could be chosen between 0 to 100 cm per hour. A mullite tube was used because of its thermal shock resistance. A temperature limit switch prevented accidental melting by shutting off furnace power if the temperature came too close to the melting point. Specimens were set in a graphite boat with their long axis along the direction of furnace motion so that the temperature gradient within the crystal was maximized.

D. Techniques of Direct Observation of Dislocations

Most of the experimental results in the present work have been obtained by the etch pit method. X-ray topograph pictures were also taken for some thin crystals only to see the actual dislocation structure inside the crystal and to substantiate the etch pit observations.

1. Etch Pit Technique

In theory dislocation etch pits should be formed at the intersection between a dislocation line and a crystal surface, because the chemical

potential should be higher at and near a dislocation core. Therefore, when a crystal with dislocations intersecting the surface is immersed in certain etchants, the points of intersection may be preferentially etched.

Chemical dislocation etch pit techniques for copper have been developed by Lovell and Wernick,¹⁸ Young,¹⁹ Livingston²⁰ and other workers. Only on low index crystallographic planes have successful etch pits results been obtained. Dislocation etch pits on the {111} plane are the most reliable and give the most uniform size of pits. Almost one to correspondence between {111} etch pits and dislocation observed by x-ray topographs of the same specimen was demonstrated by Young et al.⁵ for a low dislocation density crystal (density $\leq 10^3$ cm/cm).

The etch pit observations reported here are on {111} surfaces; the etchant was that developed by Livingston¹⁹ (one part bromine, fifteen parts acetic acid, twenty five parts hydrochloric acid, and ninety parts distilled water). Etching time was 3-7 seconds. Immediately after etching, specimens were rinsed in methyl alcohol (rinsing in water before alcohol gave less satisfactory results).

Etch pits were photographed through an optical microscope: magnification = 250 \times , a white light source with a green filter and the numerical aperture of the objective lens = 0.45. Distance between etch pits were measured on the photographs with a high resolution measuring microscope (the smallest scale division was one micron). From an etch pit picture at an original magnification of 250 \times it was found to be possible to reproduce results on the distance between the centers of two etch pits in a series of separate measurements within $\pm 0.2\mu$.

2. X-ray Topography

The Bormann technique⁵ is applicable to relatively thick ($\mu t \approx 10$, μ : normal absorption coefficient, t : thickness of specimen) specimens of high perfection. In a perfect crystal, when an x-ray beam enters at the exact Bragg angle two standing wave fields are generated inside the crystal. One wave field has nodes at the atomic planes and is transmitted with little absorption; the other has antinodes at the atomic planes and is highly absorbed. The net energy flow is very nearly parallel to the diffraction planes and at the exit surface the beam splits into two, one diffracted beam and the other parallel to the incident beam. Either beam can be used for recording topographs. Any kind of lattice defect, dislocations, vacancy clusters and etc. will be seen as a shadow. The reason why this technique has been difficult to apply to copper are as follows; First, it has been extremely difficult to obtain copper single crystals with low enough dislocation density for this method⁵ (less than 10^3 cm/cm³). Secondly, it is almost practically impossible to thin down a copper crystal as thin as 0.5 mm without introducing dislocations (thickness of < 0.5 for copper is optimum for the anomalous transmission of x-rays).

In the present work, x-ray-topographs were taken for some crystals only for checking the dislocation structure inside the crystals and for substantiating dislocation densities measured by an etch pit count after thermal cyclic annealing. An (111) diffraction of Mo-K α radiation was used for all pictures. Nuclear plates G-5 (emulsion thickness 50 μ) were used and the exposure time was about 10 hours for an area of 3 cm². After films were exposed, they were soaked in water for fifteen minutes, developed in regular x-ray film developer for thirty minutes, dipped in stopper for five

minutes and fixed for one hour.

E. Punching of Prismatic Dislocation Half-Loops

It is known¹³ that if the surface of a crystal is tapped with an indenter, an indent is created along with rows of half-loops of prismatic edge dislocations. Loops move out along the $\langle 110 \rangle$ directions that are parallel to the surface.

Seitz²¹ first suggested a process by which glide loops could combine to form a succession of prismatic loops. The work done by the force on the indenter is transferred into the sum of the energies of the dislocation loops created, their frictional losses during motion and surface energy of the indent. For a small enough contact-diameter, the local stress can reach the theoretical elastic limit, though the force is very small. This is why handling or even small solid particles falling on a perfect crystal can cause an appreciable plastic damage. In the present work spherical glass beads of a diameter approximately 300μ were dropped on the (111) surface of the copper single crystals through a vertical glass tube. This indentation probably creates rows of prismatic dislocation loops along all six $\langle 110 \rangle$ directions, three of which are towards the inside of the crystal and three of which are parallel to the surface plane (Fig. 5). By a dislocation etching, the rows of prismatic half loops have revealed along the three $\langle 110 \rangle$ directions on the surface; each single half-loop is represented by a pair of etch pits. Variation of the size of glass particles and the height from which a particle is dropped give different sizes of loops.

F. Shape of Half-Loops

Since etch pits give only the sites of intersection between dislocation lines and the crystal surface, there is no way of knowing what the internal dislocation structure is from a single observation.

However, by polishing off some known thickness of a surface layer and by taking repeated etch pits pictures of the same dislocation loop at each successive depth until the bottom of the half-loop is reached, a crude three dimensional picture of the half-loop can be constructed.

A parallelepiped specimen was lacquer-coated, except for a known area on the (111) face, and electro-polished. The thickness of the layer removed was calculated from the weight loss. The weight was measured by the automatic analytical balance, which has an accuracy of ± 0.1 mg. The thickness of the layer removed by each electro-polishing was several microns.

G. Glide of Half-Loops

The critical shear stress to cause a half-loop to glide was estimated by making use of Bullough and Newman's equation¹¹ for the shear stress on its glide cylinder and measuring the spacing between half-loops. The total stress on the end loop due to the others in the same row should be equal to the lattice friction stress (critical shear stress) necessary to move the loop along its glide cylinder. Critical shear stress: τ_c

$$\tau_c = \sum \tau_i + \sum \tau_j \quad (\tau_i: \text{contribution of } i\text{-th loop}) \quad (1)$$

$$\tau_i = \frac{V_i \mu b}{4\pi (1-\nu) a_i} \quad (\text{when } Z/a \leq 2.5) \quad (2)$$

$$\tau_j = \frac{3b \mu a_j^3}{(1-\nu) Z_j^4} \quad (\text{when } Z/a \gg 2.5) \quad (3)$$

where:

- μ : shear modulus
- a: loop radius
- b: Burger's vector
- Z_j : distance between the loop under consideration and j-th loop
- ν : Poisson's ratio
- V: constant depends on Z/a obtained from graph computed by Bullough and Newman (V increases as Z/a decreases).

When the distance between two loops is large compared with their radius, the force between them varies as Z^{-4} so only the first and second neighbors are important. Bullough and Newman's analysis applies strictly only to complete prismatic loops, but the loops studied here were half-loops at a surface. Therefore it has been assumed that Bullough and Newman's calculations will be approximately valid for surface half-loops. The shear stress across a plane, normal to the plane of a prismatic edge dislocation loop and through its center is zero. The normal stress across the same plane is not zero, but is small for large loops. Therefore cutting the crystal along such a plane should not greatly change the shear stress distribution along the glide cylinder.

By annealing rows of loops of different sizes, information on critical shear stress for glide-size of loop was obtained. Twisting motion of half loops under the action of a bending stress was also studied by applying bending loads around the $\langle 112 \rangle$ axis of the specimen (see Fig. 2). A device was made for the bending tests, using an analytical balance; loads can be applied with an accuracy of one milli-gram.

H. Climb of Half-Loops

Indentation punched prismatic edge dislocation half loops are interstitial type and therefore, they shrink by absorbing vacancies. Vacancies can be supplied both by diffusion through the bulk and along the dislocation line.

Shrinkage rate of loops were obtained at three different temperatures. Figure 6 shows the apparatus for the diffusion study. It was essential for the study of diffusion by the etch pit method that heating and cooling of the specimen should be done quickly without surface oxidation or contamination. In order to achieve a quick heating and cooling, first, the furnace was heated up and then the specimen was inserted from the top of the tube. During the insertion process argon gas was made to flow upward in the tube to minimize surface oxidation of the specimen. After the top was closed and sealed, the argon flow was stopped and a downward helium gas flow was started. Temperature and time were recorded automatically on charts. After annealing for a desired period of time, the furnace power supply was shut off and the tube was cooled down to room temperature in a cold blast of air. A temperature-time curve is shown in Fig. 7. Annealed specimens generally maintained good surface conditions. They were, if necessary, electropolished for 15-30 seconds, to provide a clean surface for dislocation etch pit formation. This process of annealing and dislocation etching was repeated so that the shrinkage rate could be obtained by measuring at each stage the distances between a pair of etch pits on photographs. From the shrinkage rate-annealing time curves, the apparent activation energy for the climb process was estimated.

III. RESULTS

A. Effects of Thermal Cyclic Annealing

Specimens had an average dislocation density of $10^5 \sim 10^6$ cm/cm³ in the as-grown state. Very few subgrain boundaries were observed. After specimens were annealed under cyclic change of temperature the average dislocation density over the entire specimen area was reduced to $\leq 10^3$ cm/cm³ as shown in the etch pit picture (Fig. 8). Dislocation populations as low as 0 to 50 cm/cm³ were observed in certain areas (as large as 0.5 cm²). A few transmission x-ray micrographs were taken (Fig. 9) which confirmed the low dislocation density.

Since the study of annealing mechanisms under cyclic changes of temperature was not the author's main interest, detailed investigation of the effects of (annealing) variables were not carried out. However, annealing times were varied from 100 hours to 200 hours. The decrease in dislocation density seemed to saturate after an annealing time of about 150 hours. Specimens containing subgrains still contained subgrains even after annealing.

B. Prismatic Dislocation Half-Loops

Rosettes of prismatic dislocation half-loops were introduced by dropping spherical glass particles (300 μ diameter) on the (111) surface of specimens from several different height depending on the desired size of loops. A rosette pattern of quite regular shape is shown in Fig. 10. Each of the six branches of a rosette, extending along different $\langle 110 \rangle$ crystallographic directions, consists of a row of prismatic edge-dislocation half-loops. A pair of triangular pits represents the two intersections between the

surface and the two ends of a half-loop of pure edge dislocation. When a glass particle hit the surface at an angle other than 90° , it causes several rosettes, the sizes of which became smaller as the maximum height of the bouncing particle decrease (Fig. 11).

C. Geometry of Etch Pits

The three sides of the triangular dislocation etch pits are along the three $\langle 110 \rangle$ directions. There are two different combinations of $\langle 110 \rangle$ which make equilateral triangles on a $\{111\}$ plane, either a-1 or a-2 in Fig. 12. In order to know which of the two is the case, an optical microscope picture of a pitted surface and an x-ray Laue back-reflection picture of the same specimen from the same direction were compared. Tetrahedron of $\{111\}$ planes is also shown in Fig. 12. From the analysis of Laue spots, it was found that the pyramidal planes of an etch pit were tilted relative to the surface in the same direction as the three intersecting $\{111\}$ planes.

D. Shape of Half-Loops

Before climb and glide of loops were studied, the initial shape of loops under the surface was examined by successively etching and polishing off surface layer, (Fig. 13). The amount of material taken off in each step was calculated from the weight loss after polishing. Typical plots of the distance between a pair of pits and the depth from the surface (Fig. 14-b) are shown for both as-punched (Fig. 14a) and as-annealed at 550°C . There was no appreciable change in microscopic shape within plus or minus a few microns after annealing at a high temperature. Approximately symmetrical semicircular shapes were always observed.

E. Glide of Prismatic Dislocation Half-Loops

By making use of Bullough and Newman's approximation,¹¹ critical shear stresses for glide of prismatic half-loops of different sizes were calculated. Rows of loops chosen for calculated were those that were of regular and uniform shape and did not have any obvious obstacles ahead on their $\langle 110 \rangle$ directions or any unpaired along the row which might give rise to long stresses on the dislocation loop under consideration. The critical shear stress acting along the glide cylinder at the position of the last loop of a row was calculated as the sum of shear stresses due to its first, second and third neighbors ($\tau = \sum_{i=1}^3 \tau_i$). A sample calculation is shown in the Appendix.

Critical shear stresses were calculated for a series of loops of different size as punched out, and also, after being annealed at 550°C for thirty minutes. The latter should give the critical shear stress required for glide at 550°C. Plots of $\tau_{\text{crit}} - 1/r$ are shown in Figs. 15 and 16 and examples of etch pit pictures of rows of loops of different sizes are shown in Fig. 17. τ_{crit} represents an upper limit for the true critical shear stress, because it was assumed that the specimen crystal was perfect except for prismatic dislocations. From Fig. 15 and 16 ($\tau_{\text{crit}} - 1/r$) it is observed that τ_{crit} increases when the size of the half-loop decreases (that is, the greater the curvature of the dislocation, the greater force needed to move it) and τ_{crit} decreases as temperature increases, implying that glide involves thermally activated escape of the dislocation from barriers. Figure 18 shows the effect of applying a bending stress. The twisting motion of some half-loops were revealed by etching before and after loading. When the size of a loop is relatively large, interaction between opposite sides in a half-loop is weak.

The two ends intersecting the surface act almost like isolated individual straight dislocation lines. Figures 18d and 18e show motion of the two sides in the opposite directions and Fig. 18f shows twistings in the opposite directions, when stress was first applied, the loop twisted in one direction (see the pair of etch pits of the middle size) and when the stress reversed, it twisted in the opposite direction (see the smallest pits). Figure 18a, b and c are the examples where only one side of the half-loops moved under the shear stress, while the other sides were pinned.

F. Climb of Prismatic Dislocation Half-Loops

The prismatic dislocation half-loops studied were of edge character and of interstitial type. It was possible to make the loops shrink by dislocation climb if a specimen was heated to a high enough temperature for vacancy diffusion to take place. The shrinkage rate was measured for three different temperatures namely at 625°C, 645°C and 675°C and an apparent activation energy for shrinkage a loop was calculated. A nearly parabolic relation between the radius of a half-loop and the annealing time is shown in Fig. 19.

Considering the relatively poor resolution of the technique, the average value of the shrinkage rate, $P = r^2/t$ (r is the radius and t is the annealing time), for a given temperature was obtained from the measurements of several loops, namely $P(T) = 1/n \sum_{i=1}^n P_i$.

The least-square method has been utilized for obtaining the slopes. Figure 20 shows the $\log P-1/T$ curve. The slope of the curve was also obtained by the least squares method. The error limits of the plots in Fig. 20 show the limits of scatter due to different loops. The apparent

activation energy(E) of shrinkage and the slope of the log P-1/T curve are related by the equation; $E = -2.303 k \times (\text{slope})$ where k is the Boltzmann's constant. From the analysis the apparent activation energy $E = 1.28 \pm 0.30$ (eV) was obtained.

The error limit of the activation energy (E) was estimated from the maximum and the minimum possible slope of log P-1/T curve within the error ranges of $P(T) = (r^2/t)$.

IV. DISCUSSIONS

A. Shape of Half-Loops

From Fig. 14 it is clear that the punched-out half-loops were macroscopically not rhombus shape with side on {111} planes (Fig. 21b) as is the case where this is a more marked preference for the close packed plane, but approximately semicircular, which requires the dislocation to be jogged on a microscopic scale.

On an atomic scale the edge of the extra half plane of atoms must have numerous steps. The model of a half-loop shown in Fig. 22 will be assumed for the following discussion. The fact that half-loops were approximately semicircular instead of rhombus shape is of interest in connection with their mechanisms of formation.

In the present experiments no prominent change in macroscopic shape were observed even when loops were annealed at a high temperature (Fig. 14b). At this temperature diffusion is rapid. This suggests that loop energy would not be significantly reduced if the loop were to adopt a more angular shape. On the microscopic scale below the resolution of the etch pit technique, half-loop may have steps of different sizes depending on loop size. This might be expected from a consideration of the mechanisms through which a dislocation half-loop is formed and punched out during an indentation.

If a hard ball is dropped on the specimen surface, the maximum shear stress arises at some distance below the contact surface, according to the theory of elastic contact between spheres developed by Herz and Föppl (a flat plane is regarded as a sphere with the radius = ∞).

Figure 23 shows a possible situation near the point of indentation seen from $\langle 110 \rangle$ direction. It is reasonable to assume that a plastically deformed region will be formed underneath the contact surface with the glass ball surrounded by an elastically deformed region. In this situation dislocation half-loops are formed and punched-out in order to release the stored strain energy. A reasonable mechanism of loop formation is that a small dislocation loop is first formed somewhere on a $\{111\}$ plane in the heavily stressed region with its Burgers vector $a/2 \langle 110 \rangle$. The screw component of the loop would then tend to sweep around the half spherical stress contour by a number of successive cross slippings, which may not be confined to $\{111\}$ planes, forming a pair of prismatic loops; an interstitial half-loop and a vacancy half-loop. The interstitial loop glides away along a $\langle 110 \rangle$ direction and the vacancy loop is annihilated within the plastically deformed region. The shape of the loop formed should depend largely on the stress contour and the stress gradient, and so larger loops should tend to contain longer steps resulting from less frequent cross slippings.

For simplicity of discussion it will be assumed that average length of steps (l_j) is proportional to the loop radius (r), namely $l_j = pr$ and that p is a function of temperature (Fig. 24).

B. Glide of Half-Loops

The critical shear stress (τ_c) for loop motion increases rather monotonically with the reciprocal of the loop radius (Fig. 15) and τ_c decreases when annealed at a high temperature (Fig. 16). These observations suggest that the density of pinning points along the dislocation is a function of the loop of radius and annealing history.

Possible dislocation pinning mechanisms are:

1. Pinning by impurity atoms or vacancy clusters
2. Long range stress by grown-in dislocations
3. Surface pinning due to surface roughness
4. Pinning at steps on the dislocation line.

Pinning by foreign atoms has reported to be important even for high purity copper (99.999% Cu).

Young¹ explained the observed critical shear stress of 4g/mm^2 for grown-in dislocation in 99.999% Cu in terms of a Cottrell atmosphere. He observed that fresh dislocation moved at a critical shear stress lower than 4g/mm^2 . However, there are other possible differences between grown-in and freshly multiplied length of dislocation, one of which is a difference in jog density.

It is difficult to see how impurity pinning could explain the size effect observed in the present experiments; the short range interaction between a solute atom and a dislocation should not be sensitive to its macroscopic radius of curvature. Pinning by vacancy clusters is subject to the same objection. The x-ray transmission topograph of an annealed sample shown in Fig. 9 has dark spots which, according to Young,⁶ presumably are due to vacancy clusters. The density of these spots is comparable with the density of dislocation etch pits. Therefore it does not seem likely that these could have been the primary barriers to dislocation glide.

The long range elastic stress due to grown-in dislocations is negligible in the highly perfect crystals used for the present study (The density was less than 10^3 cm/cm^3 and over area larger than the indentation rosettes

the crystals were often dislocation free). Any contribution from internal stresses to the critical shear stress for glide of half-loops would also be independent of loop size.

Pinning of the end of the dislocation at the crystal surface could make a size dependent contribution to the critical shear stress. On an atomic scale even a carefully electropolished metal surface has some surface roughness. An α -brass surface carefully electropolished in a phosphoric acid solution has a surface roughness of 20-100Å.²³ When a dislocation intersecting a crystal surface glides, it is necessary that a new surface area is created along the path of the dislocation wherever the Burgers vector has any component at right angle to the surface. Also some change in the dislocation length may occur. A microscopic view of a (111) plane with some roughness is expected to be something like Fig. 25. Therefore the applied stress has to supply extra energy for the newly created surface area when the dislocation moves.

Consider glide of a half-loop from a dynamical point of view. The situation will be such that a half-loop at the end of a row in a rosette during and after the indentation has been made is acted upon by a stress equal to the sum of the stress field of all the half-loops behind it tending to make it continue to glide along its glide cylinder. Its velocity will have been much higher just at the time of the impact which caused the row of loops to be punched out, but it must only gradually slow down as the net stress acting on the loop becomes smaller as the distances between loops in the row become larger. It is assumed that at the moment of observation, which is at least a few hours after loops were punched out, the velocity of the outermost loop in a row has become so small that the

displacements over a limited period of time (even for weeks) is not enough to be detected by a dislocation etch pit method. For a dislocation held at atomic scale pinning points, the velocity of glide can be expressed as:¹³

$$V = a v_0 \exp\left(-\frac{W - \sigma b l a}{kT}\right) \quad (4)$$

where.

a = distance moved for each thermally activated event

v_0 = frequency of vibration of the dislocation segment

W = energy to escape from pinning points

σ = applied stress

b = Burgers vector

l = distance between pinning points

The contribution of surface pinning can be roughly estimated by substituting appropriate quantities in the above equation. Taking surface energy (γ) as 1800 erg/cm^2 , $W = \gamma b^2 = 0.7 \text{ eV}$, $T = 300^\circ \text{K}$, $v_0 = 10^8/\text{sec}$, $b = 2.5\text{\AA}$, $\sigma = 5\text{g/mm}^2$, $a = 10^2 b$ and $l = 16\mu$ for a loop of a radius 10μ one obtains $V = 10^{-2} \sim 10^{-3} \mu/\text{sec}$. Therefore the loops are not being held back primarily because of surface pinning.

In Section A the shape of the half-loops was described macroscopically as semicircular with jogs or steps which were assumed to exist when the dislocation changed from one glide plane to another (Fig. 22). For such a dislocation the core energy at jogs or at the ends of superjogs might be expected to be higher than that in straight segments on $\{111\}$ planes. Consider the atomic configurations at corners of steps: Fig. 26 shows two different kinds of corners, one is of acute angle, LMN, and the other of the obtuse angle, PQR, corresponding respectively to corners of the

heavily stepped side and the less stepped side of a dislocation half-loop.

It seems unlikely for a dislocation line to have atomically sharp corners as LMN or PQR in Fig. 26. It requires the difference in energy between dislocations lying on $\{111\}$ planes compared to on other planes to be unreasonably large. Therefore it is expected that the dislocation will shorten its length by rounding corners as $LMN \rightarrow LN$ or $PQR \rightarrow PR$. By rounding of corners on an atomic scale the segment of dislocation LN will be approximately on a $\{100\}$ type plane while PR will be on a $\{110\}$ type plane. Both $\{100\}$ and $\{110\}$ planes are relatively densely populated planes of atoms. It will be assumed that a length equal to five Burgers vectors is on a plane other than $\{111\}$; $LN \approx PR \approx 5b$.

If every corner of each step on half loops of different size has the same atomic configuration, the size effects on the critical shear stress for glide of half loops can be explained qualitatively.

Figure 29 shows schematic pictures of a large and a small step with rounded corners. When the step lengths get shorter, as is probably the case for smaller half-loops, the fraction of total dislocation length which lies on planes other than $\{111\}$ increases. For smaller loops a greater fraction of the dislocation line is forced to glide on $\{110\}$ or $\{100\}$ rather than on $\{111\}$ requiring a higher stress. Glide on nonclose packed planes is expected to be associated with a higher Peierls-Nabarro stress. The critical stress for motion would be expected to be temperature dependent.

C. Minimum Energy Configuration of Half-Loops

It is expected that, for a prismatic dislocation loop, the orientation for minimum energy will not be that of the shortest total dislocation length which is the pure edge orientation, but will be an orientation that is tilted on the glide cylinder due to the interactions between opposite segments.

Bullough and Forman²⁴ have considered the orientation dependence of the elastic strain energy of a rhombus shaped dislocation loop quantitatively.

Energy variations accompanying rotations about $\langle 110 \rangle$ and $\langle 001 \rangle$ axes were computed. Their results show that a shallow minimum in the energy exists away from the pure edge orientation for a large range of loop sizes. The sizes of loops studied in the present experiments are such that $10^3 < a/r_0 < 10^5$ (a = diameter of loop, r_0 = radius of dislocation core). Bullough and Forman's results show that the energy of a loop in this size range does not change much when it is rotated within $\pm 20^\circ$ about either a $\langle 110 \rangle$ or an $\langle 001 \rangle$ axis.

This could explain the observed scatter in the orientation of half-loops. Only frictional stress must be overcome to rotate a half-loop within about $\pm 20^\circ$ away from the pure edge orientation.

Therefore the tilt of a particular set of loops probably depends on the stress distribution that existed when the loops were being punched out. There are always some irregularities of the surface of the crystal and of the glass beads used for indentation. Therefore the stress field should seldom be exactly symmetrical.

Grown-in defects, both point defects and dislocations may also serve as obstacles to the gliding half-loops and can cause rotation away from the pure edge orientation.

D. Twist of Half-Loops in Glide Cylinder

In this section mobility of a jogged dislocation is discussed. A large half-loop is in some respects like a pair of edge dislocations of opposite sign intersecting a crystal surface.

According to the half-loop model in Fig. 22 dislocation - α (ABCD:---) is expected to have more jog steps than dislocation - α (A'B'C'D'---). Under the operation of a bending stress with the bending axis along $\langle 112 \rangle$ (see Fig. 2) the dislocation- α and the dislocation- β are expected to move in opposite directions along the glide cylinder. If jog steps act as pinning points, the dislocation- β should be more easily moved because it has fewer steps.

Various examples are shown in Fig. 18, where the dislocation- β has moved while the dislocation- α has not moved under the same stress.

This result is further evidence that jog or step density is an important factor in determining mobility of an edge dislocation.

Figure 18h suggests an interesting case in which a dislocation of type -B was pinned at or very near the crystal surface but the applied stress was large enough to bow out the highly mobile straight segments inside crystal. Figure 28 explains what has probably happened in case of Fig. 18h (refer also to Fig. 22). The segments E'F' and G'H' appear to have bowed out in their glide planes and reached the crystal surface and split into two, leaving small surface loops A'-A'₁ and A'₂-A'₃.

These experimental results are consistent with the model for a prismatic dislocation half-loop in Fig. 22.

E. Climb of Half-Loops

Important results from the annealing studies are:

1. Indentation punched prismatic dislocation half-loops always maintained an approximately ~~semicircular~~ shape during annealing.
2. The shrinkage curve $r^2 - t$ was approximately linear (r is the radius of loop, t is the annealing time).
3. The apparent activation energy for shrinkage of loops was 1.28 eV.

In the following possible rate controlling climb mechanisms are discussed which might give a reasonable interpretation of the present experimental results.

a. Dislocation Pipe Diffusion It is generally believed that a dislocation core is a line of easy diffusion.²⁵⁻²⁸ Smoluchowski²⁵ first considered diffusion along small angle boundaries in terms of the dislocation structures of such boundaries.

Both at the core of a dislocation and at an ordinary grain boundary there are relatively open regions through which a vacancy or an interstitial atom might be expected to move with a lower activation energy than in a perfect lattice. In the present case shrinkage of a half-loop can take place by diffusion of vacancies along the dislocation core, because the two ends of the half-loop intersect the crystal surface and there vacancies can be formed. The vacancy chemical potential is different at the crystal surface compared to various points along the half-loop, which gives rise to a vacancy concentration gradient.

If the dislocation pipe diffusion mechanism is the rate controlling one, that is, if the shrinkage rate mainly depends on the rate of vacancy

diffusion along the dislocation line from the crystal surface and the dislocation is a perfect vacancy sink, it is expected that dislocation segments closer to the surface will receive a larger number of vacancies per unit time and climb faster than the bottom part of the half-loop. After some climb has occurred the shape would be expected to change from semicircular to the more elongated elliptical shape shown in Fig. 29a. The observed shape of shrinking half-loops was always semicircular and contradicts the above assumptions. The model based on the pipe diffusion as the rate controlling process also fails to predict a linear relation between r^2 and t as was observed.

Moreover, the apparent activation energy $E \approx 1.28$ eV is somewhat larger than roughly estimated values of the activation energy of pipe self-diffusion in copper. One eV or about one half of the activation energy of bulk self-diffusion is perhaps the largest reasonable value, though no one has ever accurately measured the activation energy of pipe self-diffusion in copper.

Thus the pipe diffusion mechanism does not appear to be rate controlling in this case.

b. Volume Diffusion In this mechanism, vacancies diffuse from the crystal surface into the lattice and wherever vacancies meet the dislocation they are absorbed. But this mechanism again seems unlikely to be the rate controlling one for the following reasons. The activation energy of volume diffusion is ≈ 2 eV.^{22,29} By volume diffusion it is also true that the closer the dislocation is to the crystal surface the more vacancies it should absorb and so should climb faster.

The dislocation loop might be expected to become closer to a full circle as shrinkage proceeds (Fig. 29) or at least become elongated as in Fig. 31a. This is not consistent with the present results. Quantitatively it is almost impossible to obtain a reasonably simple shrinkage equation for a volume diffusion controlled mechanism, because the diffusion paths are so complicated and the effects of the elastic stress field of the dislocation on the vacancy chemical potential would also have to be taken into consideration.

c. Vacancy Formation It seems likely from the fact that shrinking loops accurately maintain a semicircular shape, which we assume is the shape of minimum energy, that pipe diffusion is very rapid. An adequate supply of vacancies must be available at any part of the loop where the radius of curvature starts to become smaller than the average so that elongated shapes never have a chance to develop.

Since the measured activation energy for shrinkage was significantly smaller than that for volume diffusion there is a possibility that the rate controlling step could be the rate of emission of vacancies into the dislocation pipe from the point where the dislocation intersects the surface.

The idea of this mechanism is that once vacancies are produced at the intersection point of the dislocation with the crystal surface they rapidly diffuse down along the dislocation line and each point along the dislocation loop is able to absorb an equal number of vacancies per unit time. Thus the dislocation loop maintains a minimum energy configuration, a semicircular shape, throughout the climbing process. The shrinkage rate of the loop is controlled by the rate at which vacancies are produced at the special sites where the dislocation meets surface.

Assume the number of vacancies emitted per unit time (ψ) is expressed by

$$\psi = \nu \cdot n \cdot \exp - \frac{u_1 + u_2 - u_3}{kT} \quad (5)$$

where

ν : lattice vibrational frequencies

n : geometrical factor

k : Boltzmann's constant

T : Absolute temperature

$u = u_1 + u_2 - u_3$: activation energy

u_1 : energy for an atom to jump from the core of dislocation into a surface site

u_2 : atom migration energy along core of dislocation

u_3 : decrease in energy of loop per vacancy formed

The number of vacancies (N) absorbed by the dislocation loop per unit time is:

$$N = \frac{\pi r}{2} \cdot \frac{dr}{dt} / a^2 = \frac{\pi r}{2b^2} \cdot \frac{dr}{dt} \quad (6)$$

where

r : radius of loop

b : Burger's vector

$a^2 \approx b^2$: area occupied by a vacancy on (110)

t : time

In a steady state,

$$\psi = N$$

$$\frac{dr}{dt} = \frac{2b^2}{\pi r} \psi = \frac{2\nu n b^2}{\pi} \cdot 1/r \exp (-u/kT) \quad (7)$$

u_3 is a function of the loop radius r , but its value is negligibly small compared with u_1 or u_2 for the range of loop radii studied in the present work. The activation energy u , therefore, is assumed to be independent of the loop radius r . The dependency of u_3 on the radius r become important only when the loop becomes extremely small in size.

Integrating the above equation, one gets,

$$r^2 = -K t + r_0^2 \quad (8)$$

where

$$K = \frac{4\gamma n b^2}{\pi}$$

r_0 : radius when $t = 0$

Thus a parabolic relation between the radius and the annealing time is obtained.

Activation energy u_1 is the energy for the atom at the intersection of the dislocation line with the surface (atom drawn in black circle in Fig. 30) to jump on to the surface.

The possible number of sites (n) which the atoms can jump into is five (Fig. 30). In this process eight atomic bonds have to be cut and three new bond produced. u_1 is expected to be comparable to the normal vacancy formation energy in the perfect lattice $u_{fv} \simeq 1.1$ eV.

It is assumed that unless the vacancy that has been created on the edge of the extra half plane of the dislocation is filled by another atom from below during the same thermal fluctuation then it is probable that the first atom will jump back. Therefore u_2 is related to the migration energy of a vacancy in a dislocation core. This is expected to be much smaller than the migration energy of an atom in the lattice

which is less than one electron volt. The above discussion is based on the assumption that the crystal is perfect except for dislocation (perfect edge) and the surface and that the surface is parallel to the {111} plane and is nearly flat on at atomic scale.

u_3 , as mentioned already, is negligibly small and therefore, $u = u_1 + u_2 - u_3$ is expected to be between 1 - 1.5 eV which is in the range of the experimentally observed activation energy for loop shrinkage of 1.28 eV.

It can be concluded that the vacancy emission mechanism is a possible explanation of the observation experimental results on climb of surface prismatic edge dislocation half-loops.

It suggests that the dislocation core is such an easy diffusion path that a vacancy subsaturation can be maintained even at surface in the immediate vicinity of the dislocation end.

V. CONCLUSIONS

The present experiments on glide and climb of prismatic edge dislocation half-loops lead to the following conclusions:

A. Shape of Half-Loops and Glide

1. Prismatic edge dislocation half-loops with $\langle 110 \rangle$ Burgers vector were found to be macroscopically semicircular in shape. Therefore they are jogged or stepped. The step density along the length of a semicircular loop should be nonuniform. One of the two segments of a half loop near where they meet the crystal surface should have a higher step density than the other.

2. The size of steps were smaller than the resolution of the etch pit technique (i.e. less than a few microns). Considering the probable mechanism of half-loop formation, it was suggested that the average length of steps could be different depending on the size of loops, a larger loop might be expected to have a large average step length.

3. It was also suggested that corners of steps could be rounded, that is, the dislocation line is not on close packed planes at corners of steps.

4. The larger the loop the lower is the stress required to cause it to move along its glide cylinder.

5. Under applied stresses, half-loops twisted on their glide cylinders, that is, the two segments of a dislocation half-loop near where they meet the crystal surface moved in opposite directions. A higher mobility was observed for the segment that was expected to have a smaller average step density

6. From consideration of the model for the shape of half-loops and their observed behavior under the applied stress from 1 to 5, it was

concluded that mobility of dislocations under small stress is strongly influenced by step density.

B. Climb

7. Half loops decreased in size when annealed at high temperatures (625°C-675°C). Half-loops maintained an approximately semicircular shape during annealing.

8. The square of the loop radius decreased almost linearly with annealing time.

9. The apparent activation energy of shrinkage was 1.28 eV.

10. The experimental observation on shrinkage of half-loops were best interpreted by a model based on vacancy formation at the point of intersection of the dislocation and the crystal surface and pipe diffusion along the dislocation loop.

VI. APPENDIX

SAMPLE OF CALCULATION OF THE CRITICAL SHEAR STRESS TO
MOVE A LOOP USING BULLOUGH AND NEWMANS EQUATIONS

The critical shear stress of the loop is calculated as the sum of the shear stresses along the glide cylinder due to the first (τ_1), the second (τ_2) and the third (τ_3) neighbors. The geometry and sizes of the row of loops are shown in Fig. 31.

$$\tau_1 = \frac{V_1 b G}{4\pi r_1 (1-\nu)} = 3.44 \text{ g/mm}^2$$

$$\nu = 0.35$$

$$r_1 = 9.38\mu$$

$$G = 5.57 \times 10^5 \text{ g/mm}^2$$

$$b = 2.56 \times 10^{-4} \mu$$

$$V_1(\rho_1) = 0.19 \text{ obtained from Fig. 1 of Bullough and Newmans paper.}^{11}$$

$$\rho_1 = Z_1/2r_1 = 1.60 < 2.5$$

$$Z_1 = 30.0\mu$$

$$\tau_2 = \frac{3 b r_2^3 G}{(1-\nu) Z_2^4} = 0.54 \text{ g/mm}^2$$

$$r_2 = 9.38\mu$$

$$Z_2 = 56.3\mu$$

$$\rho_2 = Z_2/2r_2 = 3.0 > 2.5$$

$$\tau_3 = \frac{3 b r_3^3 G}{(1-\nu) Z_3^4} = 0.24 \text{ g/mm}^2$$

$$r_3 = 11.0 \mu$$

$$Z_3 = 78.8\mu$$

$$\rho_3 = Z_3/2r_3 = 3.58 > 2.5$$

$$\tau_c(1/r) = \sum_{i=1}^3 \tau_i = 4.22 \text{ g/mm}^2 \quad (r_0 = 9.38\mu)$$

ACKNOWLEDGEMENTS

The author wishes to express his deepest gratitude to Professor Jack Washburn for his encouragement and stimulating discussions throughout the present investigation.

He would also like to express his appreciation to Professor Hiroya Kaieda and Professor Sadakichi Kitajima for their continuous encouragement. Thanks are also given to Jane Ball and Linda LeBorgne for special efforts in typing this thesis.

This work was carried out under the auspices of the United States Atomic Energy Commission through the Inorganic Materials Research Division of the Lawrence Radiation Laboratory.

REFERENCES

1. F. W. Young, Jr., J. Appl. Phys. 32, 1815 (1961).
2. F. W. Young, Jr., J. Appl. Phys. 33, 963 (1962).
3. F. W. Young, Jr., J. Appl. Phys. 33, 3553 (1962).
4. F. W. Young, Jr., J. Appl. Phys. 32, 192 (1961).
5. F. W. Young, Jr., T. O. Baldwin, A. E. Merlini, and F. A. Sherrill, Advances in X-Ray Analysis, Vol. 9, Plenum Press, 1 (1966).
6. F. W. Young, Jr., and F. A. Sherrill, Canadian J. Phys., 45, 757 (1967).
7. F. W. Young, Jr., F. A. Sherrill and M. C. Wittels, J. Appl. Phys. 36, 2225 (1965).
8. F. W. Young, Jr., Crystal Growth (Proceedings of an International Conference on Crystal Growth, Boston, 20-24 June, 1966), 789 (1967).
9. K. Marukawa, J. Phys. Soc. Japan 22, 499 (1967).
10. P. Petroff and J. Washburn, J. Appl. Phys. 37, 4987 (1966).
11. R. Bullough and R. C. Newman, Phil. Mag. 5, 921 (1960).
12. J. Silcox and M. J. Whelan, Phil. Mag. 5, 1 (1960).
13. J. Friedel, Dislocations, Pergamon Press, (1964).
14. D. N. Seidman and R. W. Balluffi, Phil. Mag. 13, 649 (1966).
15. J. D. Livingston, Direct Observations of Imperfections in Crystals, (Interscience Publishers, New York 1962), p. 115.
16. F. W. Young, Jr., and J. R. Savage, J. Appl. Phys. 35, 1917 (1964).
17. S. Kitajima, M. Ohta and H. Kaieda, J. Japan Inst. Metals 32, 164 (1968). (In Japanese)
18. L. C. Lovell and J. H. Wernick, J. Appl. Phys. 30, 590 (1959).
19. J. D. Livingston, J. Appl. Phys. 31, 1071 (1960).
20. F. W. Young, Jr., J. Appl. Phys. 32, 192 (1961).

21. F. Seiz, Rev. Mod. Phys. 79, 723 (1950).
22. D. M. Maher, Ph.D. Thesis, University of California, (1966.)
23. P. A. Jacquet, Metallurgical Reviews, Vol. 1, Part 2, 157 (1956).
24. R. Bullough and A. J. E. Forman, Phil. Mag. 9, 314 (1964).
25. R. Smoluchowski, Phys. Rev. 87, 482 (1952).
26. D. Turnbull and R. E. Hoffman, Acta Met. 2, 419 (1954).
27. G. R. Love, Acta Met. 12, 731 (1964).
28. P. G. Shewmon, Diffusion in Solids, (McGraw-Hill, New York 1963)
p. 164.
29. H. G. Bowden and R. W. Balluffi, Phyl. Mag. 19, 1001 (1969).
30. W. G. Johnston and J. J. Gilman, J. Appl. Phys. 30, 129 (1959).
31. D. F. Stein and J. R. Low Jr., J. Appl. Phys. 31, 362 (1960).

FIGURE CAPTIONS

- Fig. 1. Established procedures of crystal growth and annealing.
- Fig. 2. Size and geometry of specimen for study of glide and climb by the etch pit method.
- Fig. 3. Apparatus for thermal cyclic annealing. The furnace moves back and forth, while specimen remains fixed.
- Fig. 4. Temperature-time chart for thermal cyclic annealing. Maximum and minimum temperatures are 1050°C and 800°C respectively.
- Fig. 5. Six $\langle 110 \rangle$ directions in which rows of prismatic dislocation half-loops are punched out. The plane of the paper is (111) .
- Fig. 6. Annealing furnace for study of climb. After the furnace was heated up to required temperature specimen was inserted from top of tube.
- Fig. 7. Temperature-time chart for annealing. Note rapid heating and cooling of specimen.
- Fig. 8. Low magnification picture of dislocation etch pits on (111) surface of an annealed crystal. Note extremely low dislocation density. Subgrain boundaries at right probably would have climbed out of the crystal if annealing time had been longer.
- Fig. 9. Transmission x-ray topograph of annealed copper. Note large dislocation free area. Dark spots probably are due to vacancy clusters. $g = \langle 111 \rangle$.
- Fig. 10. Punched out rosette of prismatic dislocation half-loops. Etch pits on (111) .
- Fig. 11. Rosettes of different sizes produced by multiple jumping of a glass bead on (111) .

- Fig. 12. Etch pit picture (b) and Laue back reflection picture (c) of the same surface from the same direction. Dislocation etch pits were found to form as in a-2. Tetrahedron of {111} is shown at ABCD. The point D is below the plane of the paper.
- Fig. 13. Etch pit pictures of a row of half-loops when the surface layer was successively removed by electropolishing.
- Fig. 14a. Two dimensional pictures of half-loops as punched out at room temperature. If one side of the loop is drawn on a {111} plane (above) then the other side does not lie on a {111} plane. Therefore the symmetrical semicircle shown below was assumed to be the actual shape.
- Fig. 14b. Two dimensional pictures of half loops as annealed at 645°C for one hour.
- Fig. 15. Critical shear stress (τ_c) vs. reciprocal of the radius of half loop ($1/r$) at room temperature. τ_c increases monotonically with $1/r$. The point represented by a square box is taken from Petroff and Washburn.¹⁰
- Fig. 16. Critical shear stress (τ_c) vs. reciprocal of the radius of half loops ($1/r$) at room temperature and at 550°C.
- Fig. 17a. Rows of prismatic dislocation half-loops of different sizes as punched at room temperature.
- Fig. 17b. Rows of prismatic dislocation half-loops of different sizes annealed at 550°C for 30 minutes.
- Fig. 18. Behavior of half-loops under a twisting shear stress. At a relatively low stress, only less jogged segments of half loops of type- β moved (a, b and c. $\tau \approx 15 \text{ g/mm}^2$). In pictures d and e, both sides of loop have moved. Segments of type- β are seen

to have moved farther. ($\tau \approx 20 \text{ g/mm}^2$). Reverse motion is observed when stress is reversed (f). One side of half-loop has moved and the other unmoved at a higher stress where appreciable dislocation multiplication has taken place ($\tau \approx 40 \text{ g/mm}^2$, picture (g)). In picture (h) dislocation is pinned at or near the crystal surface and mobile segments have swept out to surface, leaving surface half-loops. A_1-A_1' and A_3-A_3' (see also Fig. 28).

Fig. 19. Shrinkage curve r vs. t is parabolic.

Fig. 20. $\log p$ vs. $1/T$. The activation energy is obtained from the slope.

Fig. 21. Macroscopically semicircular half-loop (a) and angular half-loop (b).

Fig. 22. Model of semicircular half-loop with steps along $\{111\}$ planes. Step lengths are exaggerated.

Fig. 23. Mechanism of loop formation. Screw dislocation sweeps around spherical stress contour by multiple cross slip.

Fig. 24. Step size depends on loop size.

Fig. 25. Microscopic view of crystal surface.

Fig. 26. Corners of steps on dislocation on an atomic scale. Corners are assumed to be rounded for a distance equal to $\approx 5b$.

Fig. 27. Large and small steps - For small steps the fraction of each segment on non-close packed planes is larger than is the case for larger steps.

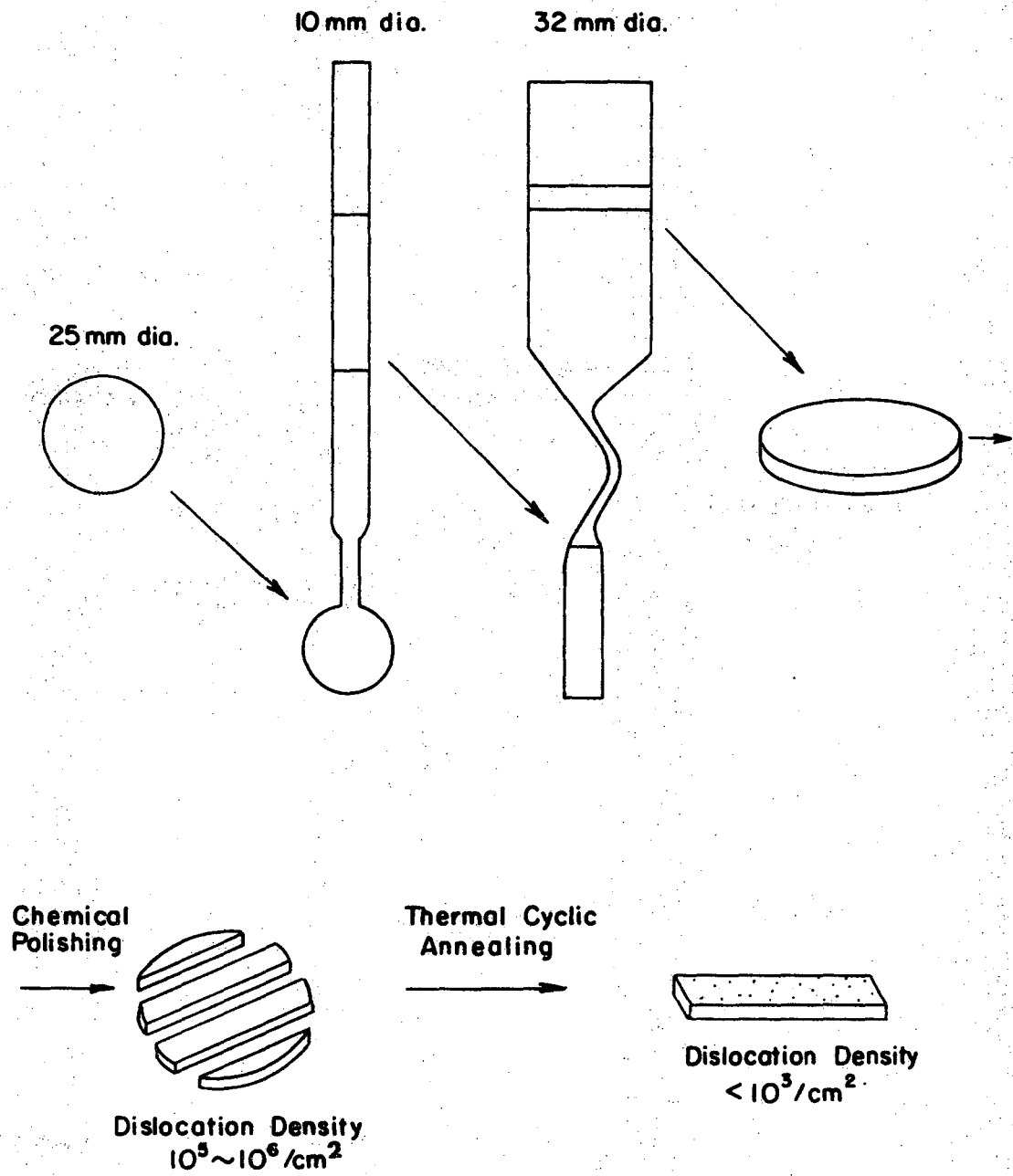
Fig. 28. Schematic picture of what has probably happened in Fig. 18h. Surface half-loops A_1-A_1' and A_2-A_2' .

Fig. 29. Possible shape of half-loops during shrinkage.

- a. Dislocation pipe diffusion controlled mechanism.
- b. Volume diffusion controlled mechanism.
- c. Vacancy emission controlled mechanism.

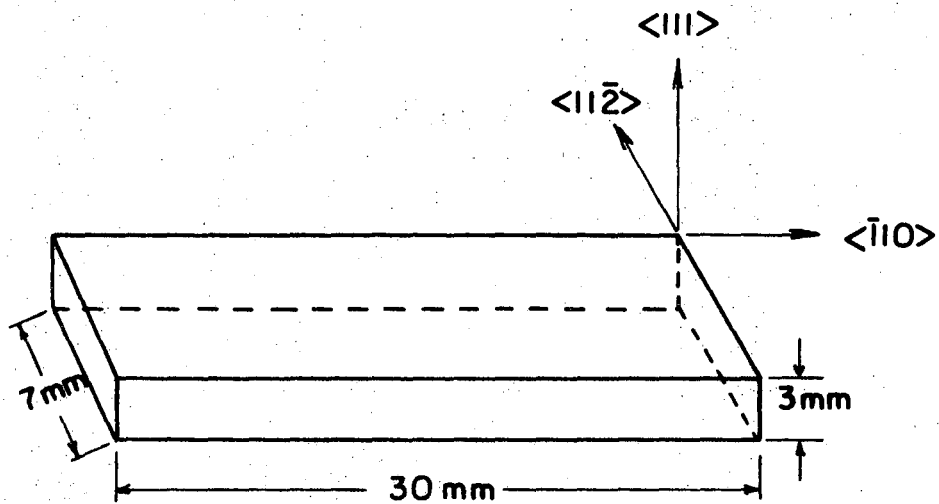
Fig. 30. View of crystal surface where dislocation meets. The atom of shaded circle can jump up to five possible different sites on surface.

Fig. 31. Schematic drawings of a row of half-loops, r = the radius of half loop and Z is distance between loops.



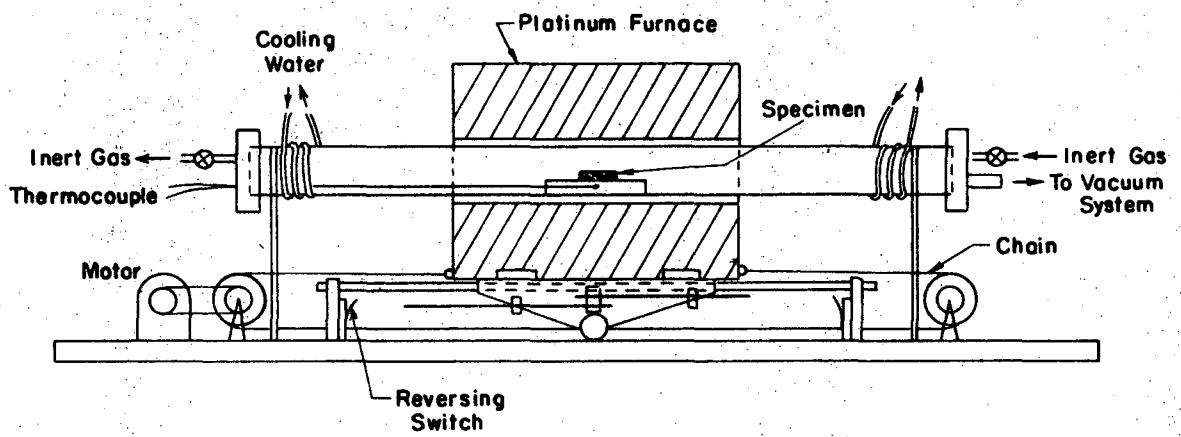
XBL 705-969

Figure 1



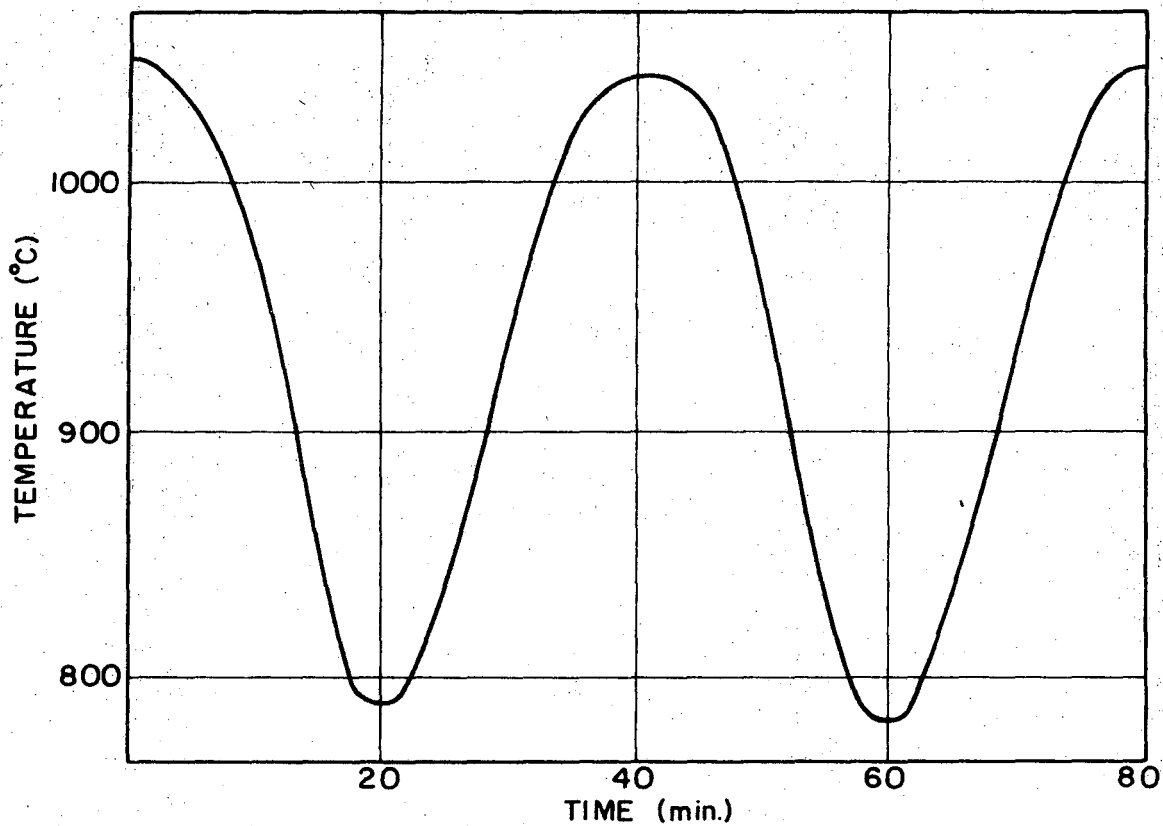
XBL 705-966

Figure 2



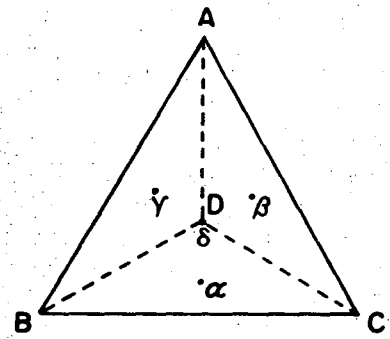
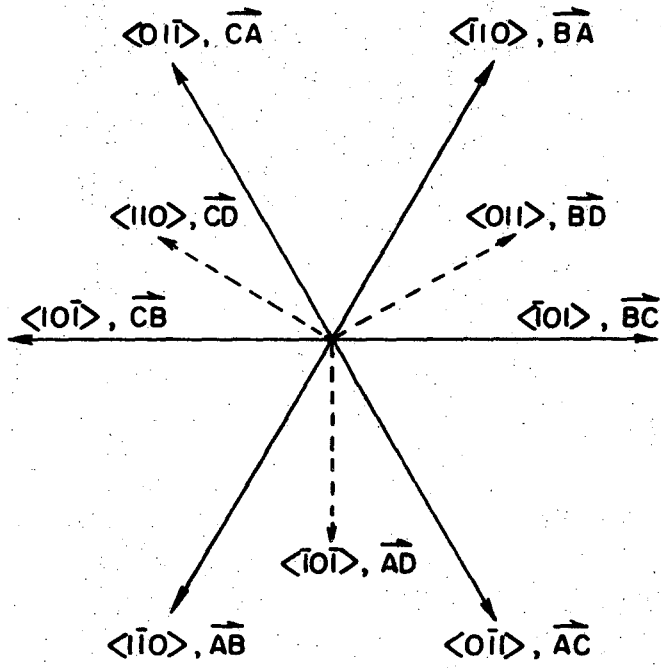
XBL 705-967

Figure 3



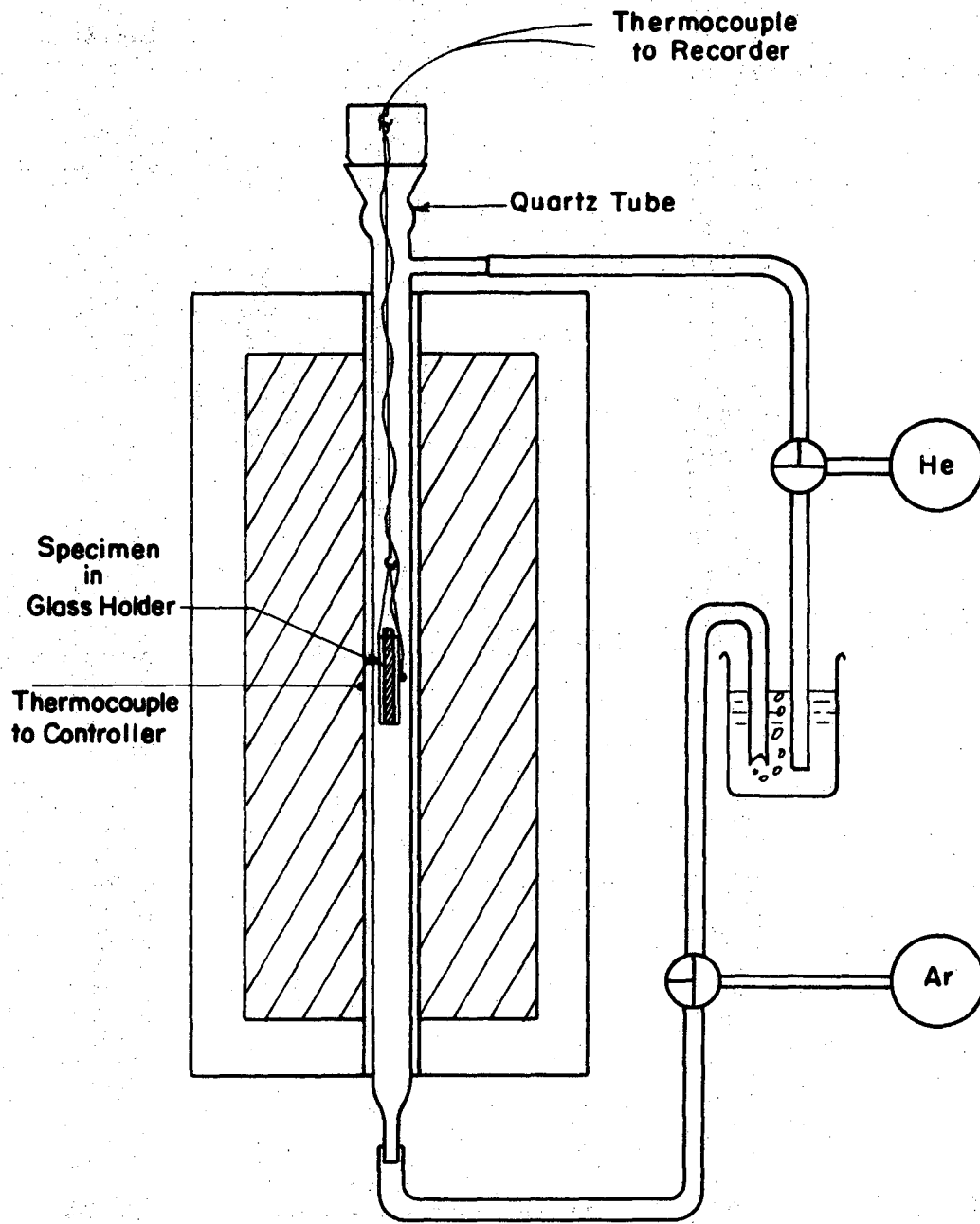
XBL 705-968

Figure 4



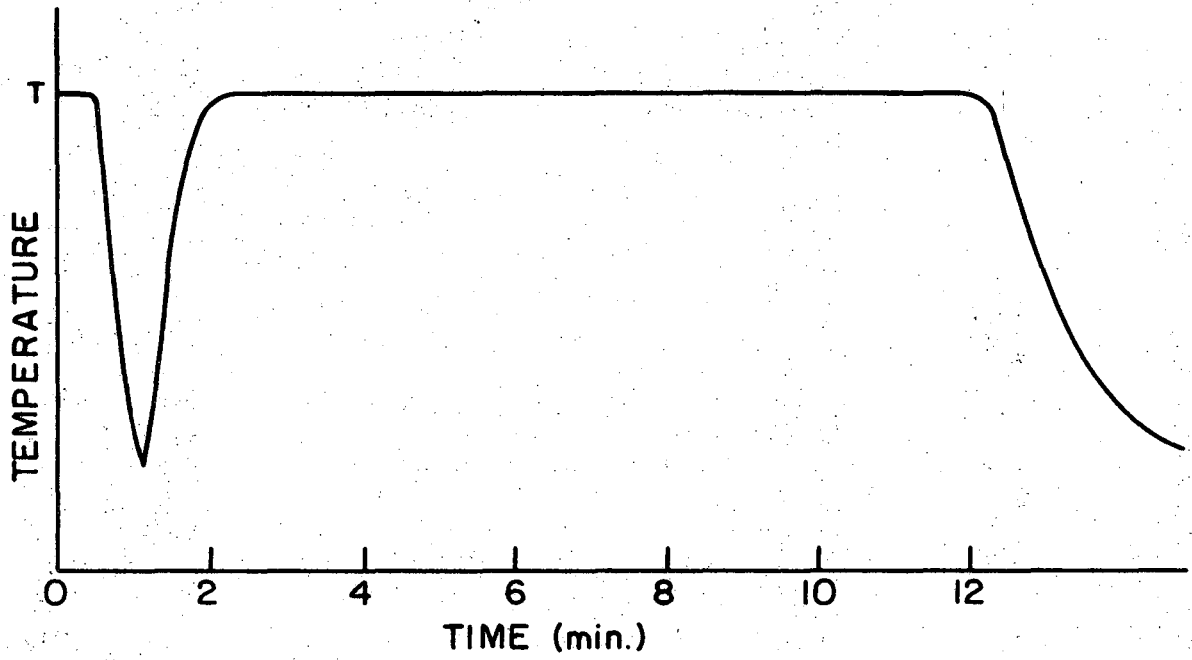
XBL 705-951

Figure 5



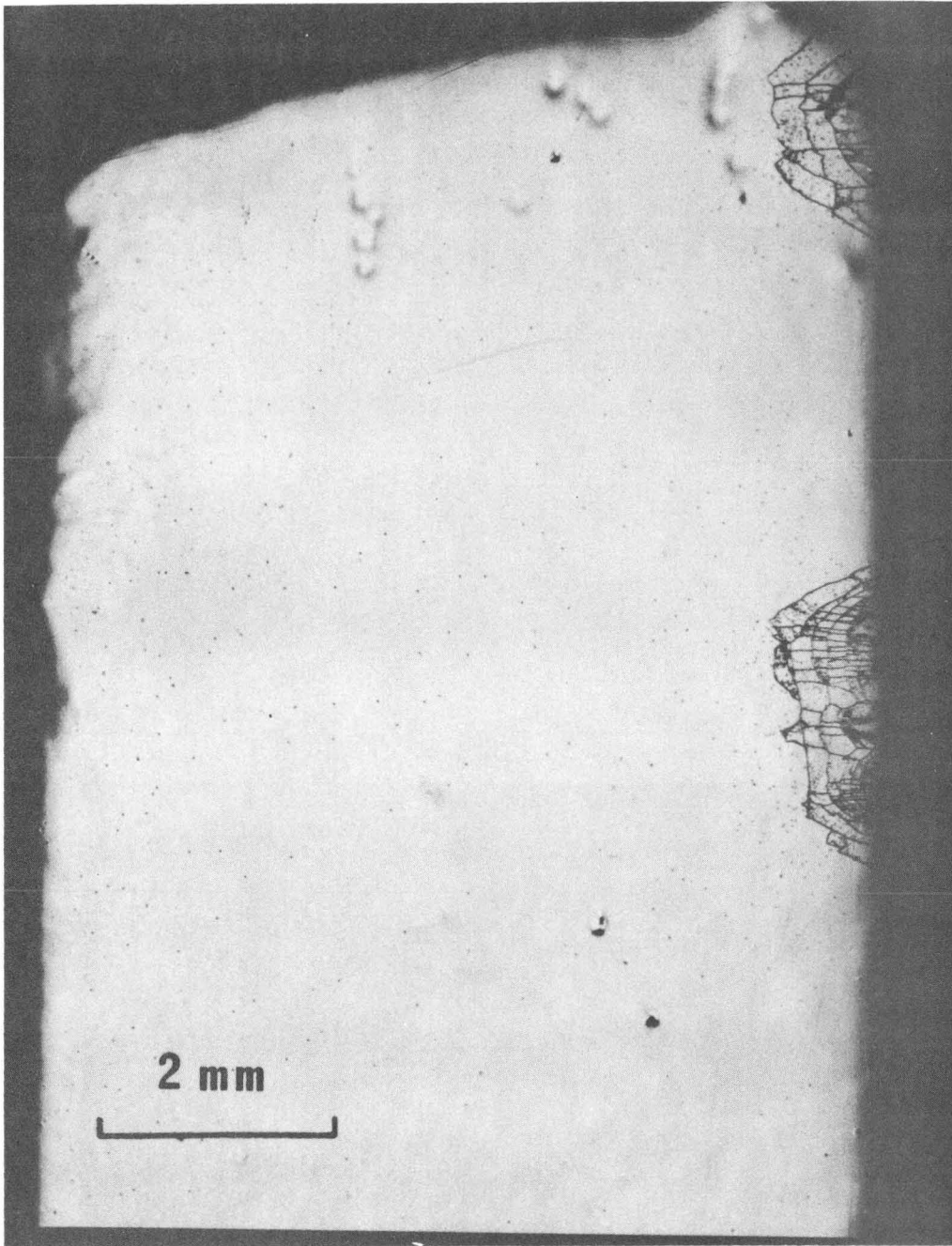
XBL 705-952

Figure 6



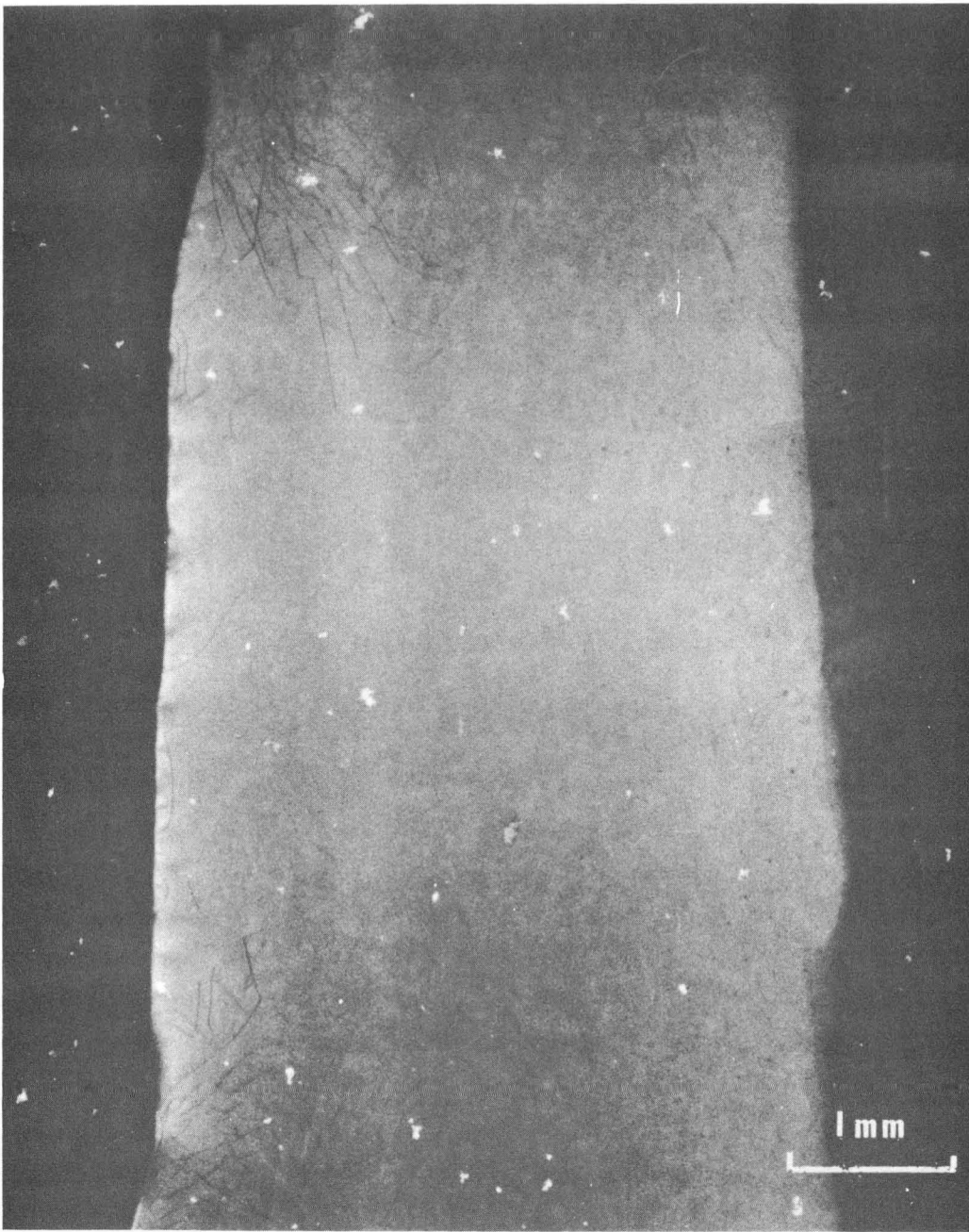
XBL 705-953

Figure 7



XBB704-1995

Figure 8



XBB704-1994

Figure 9

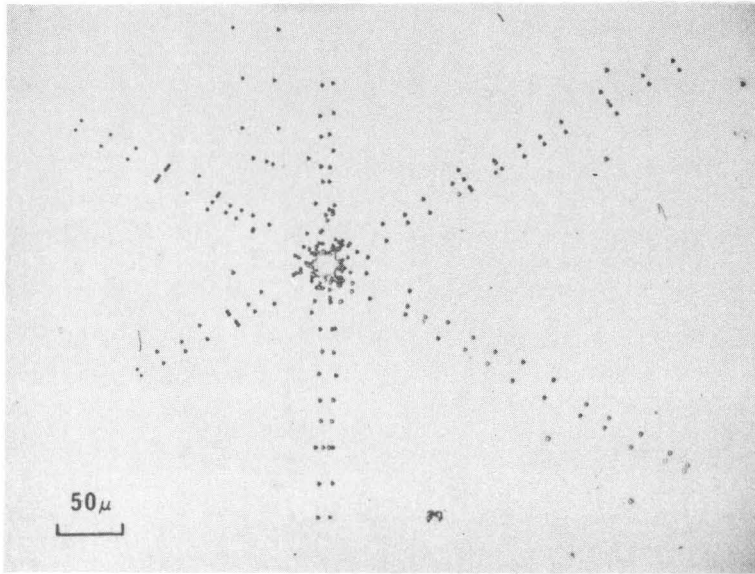
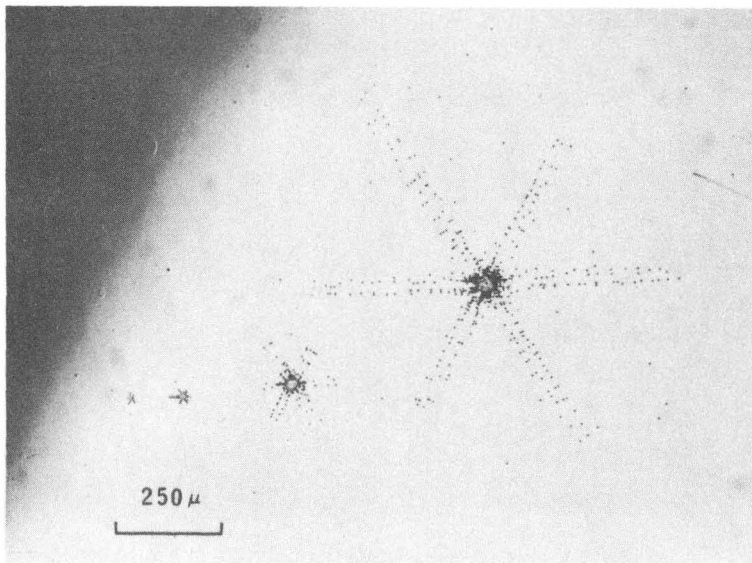
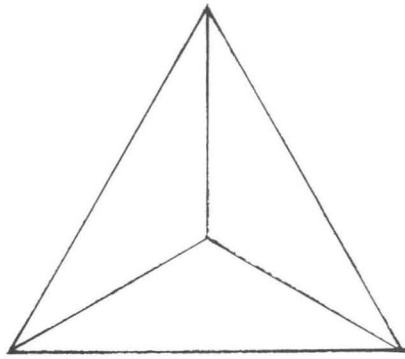


Figure 10

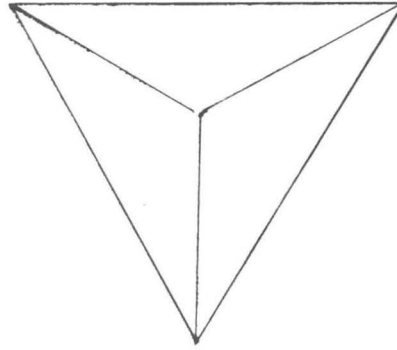


XBB704-1999

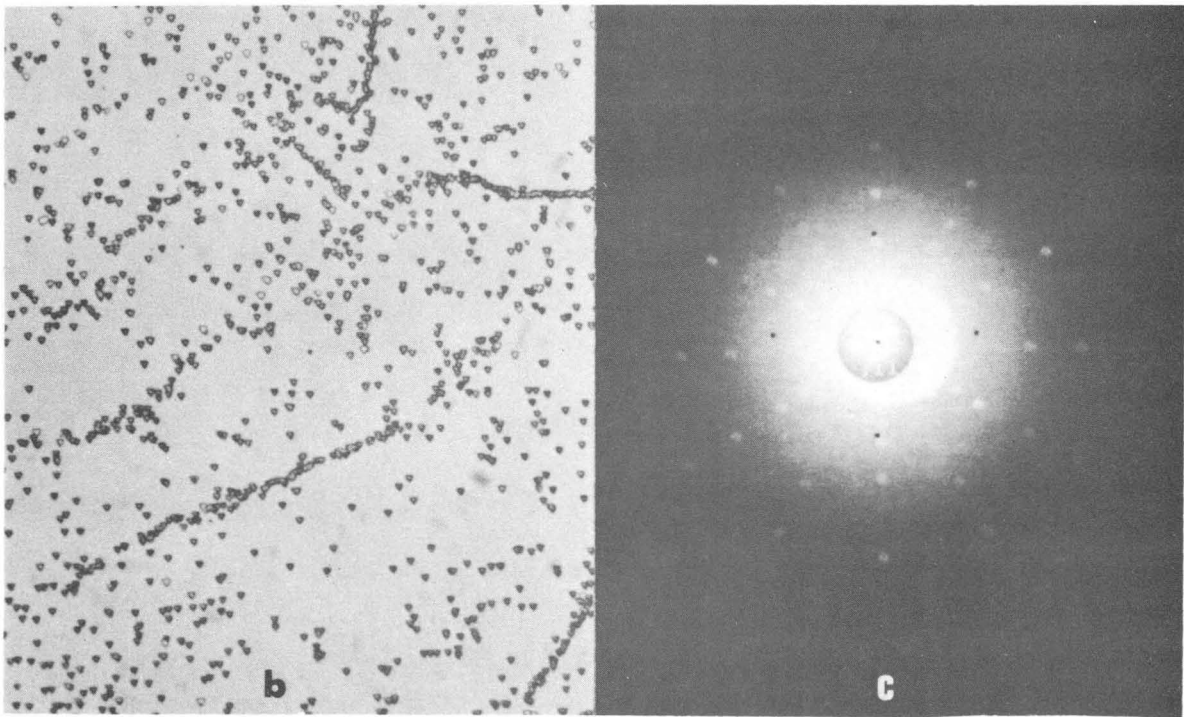
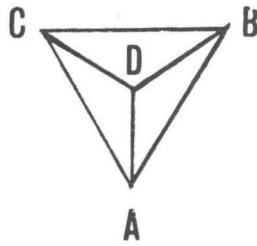
Figure 11



a-1



a-2

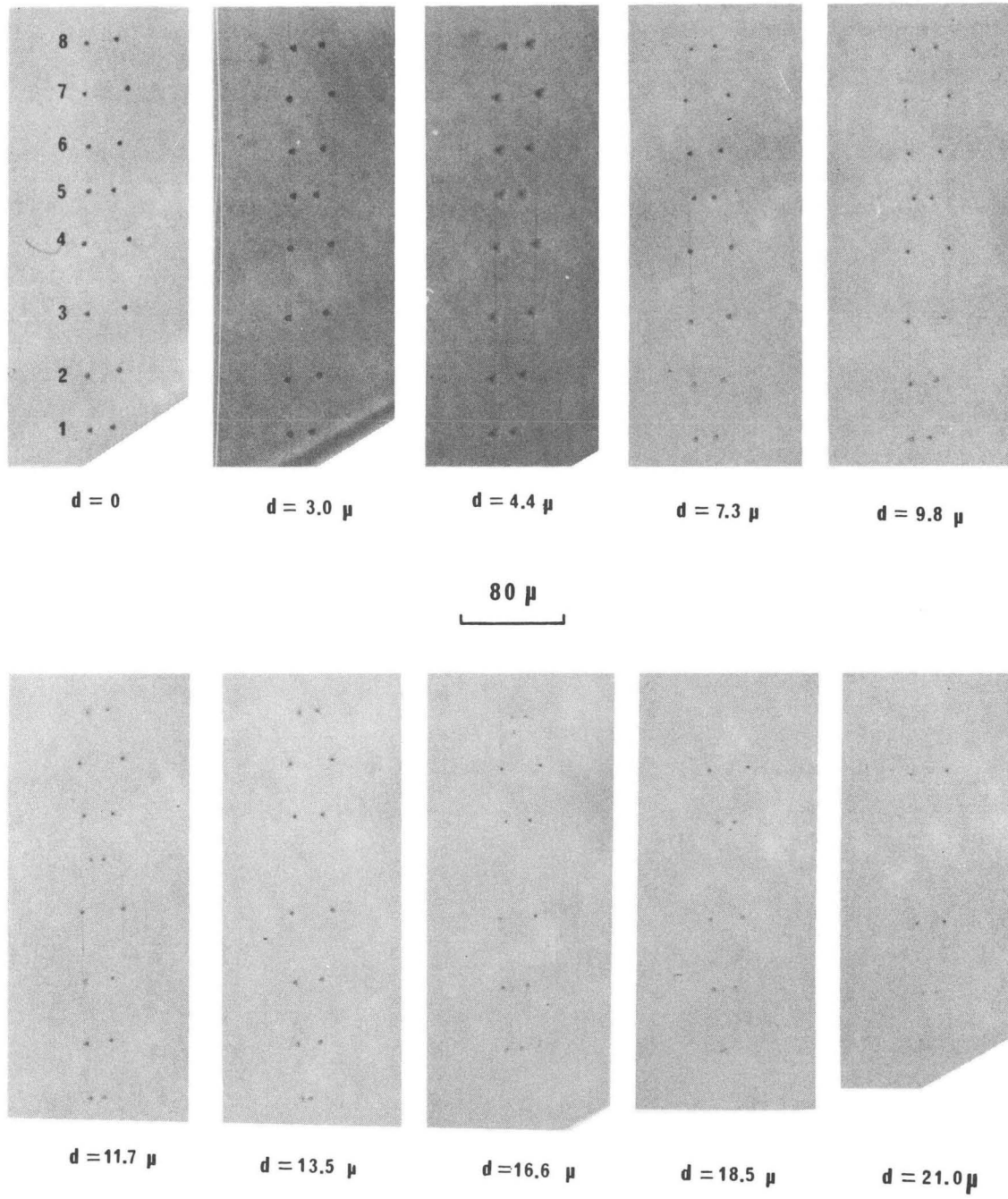


b

c

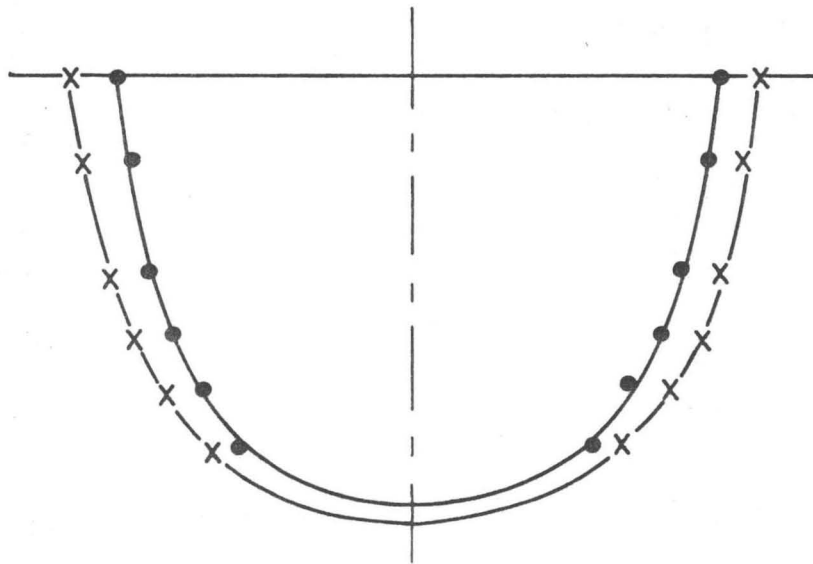
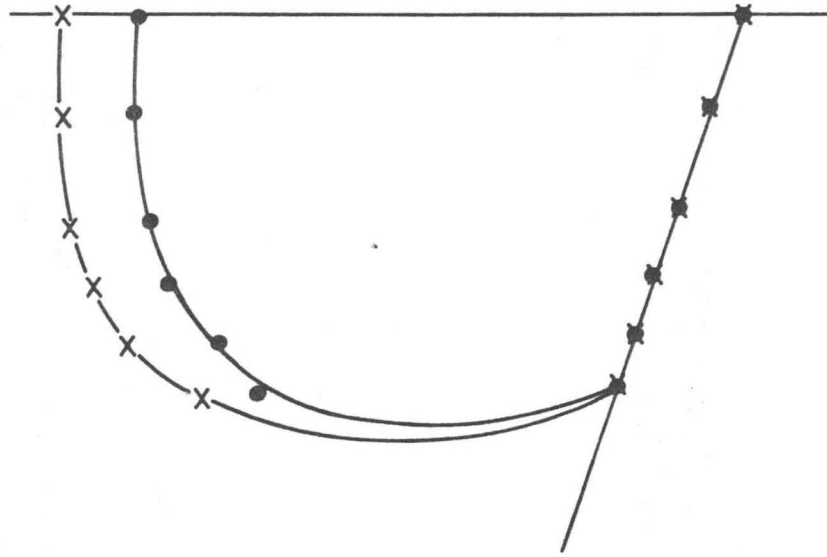
XBB704-2000

Figure 12



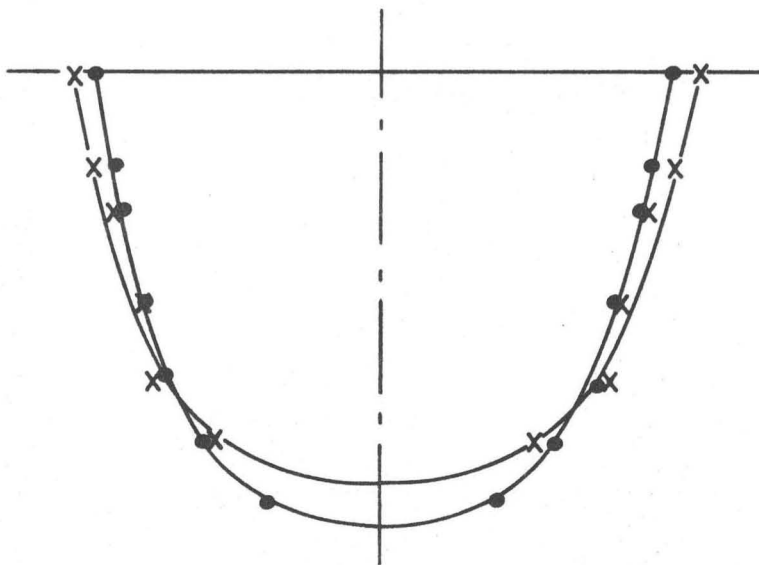
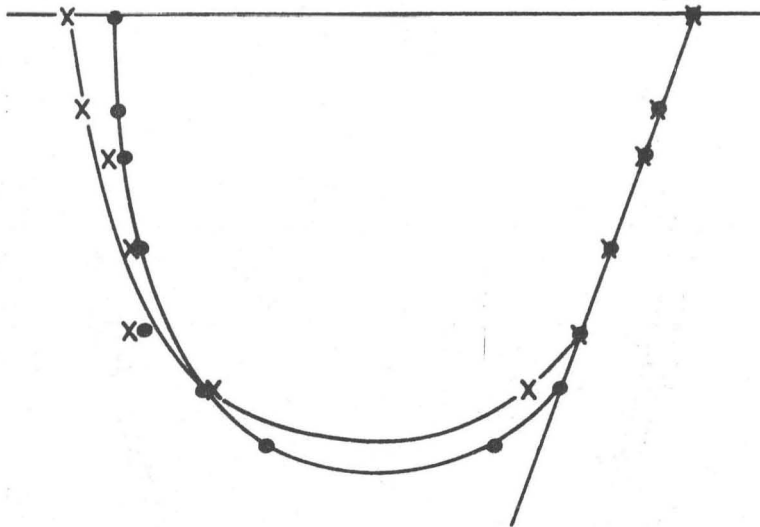
XBB704-2001

Figure 13



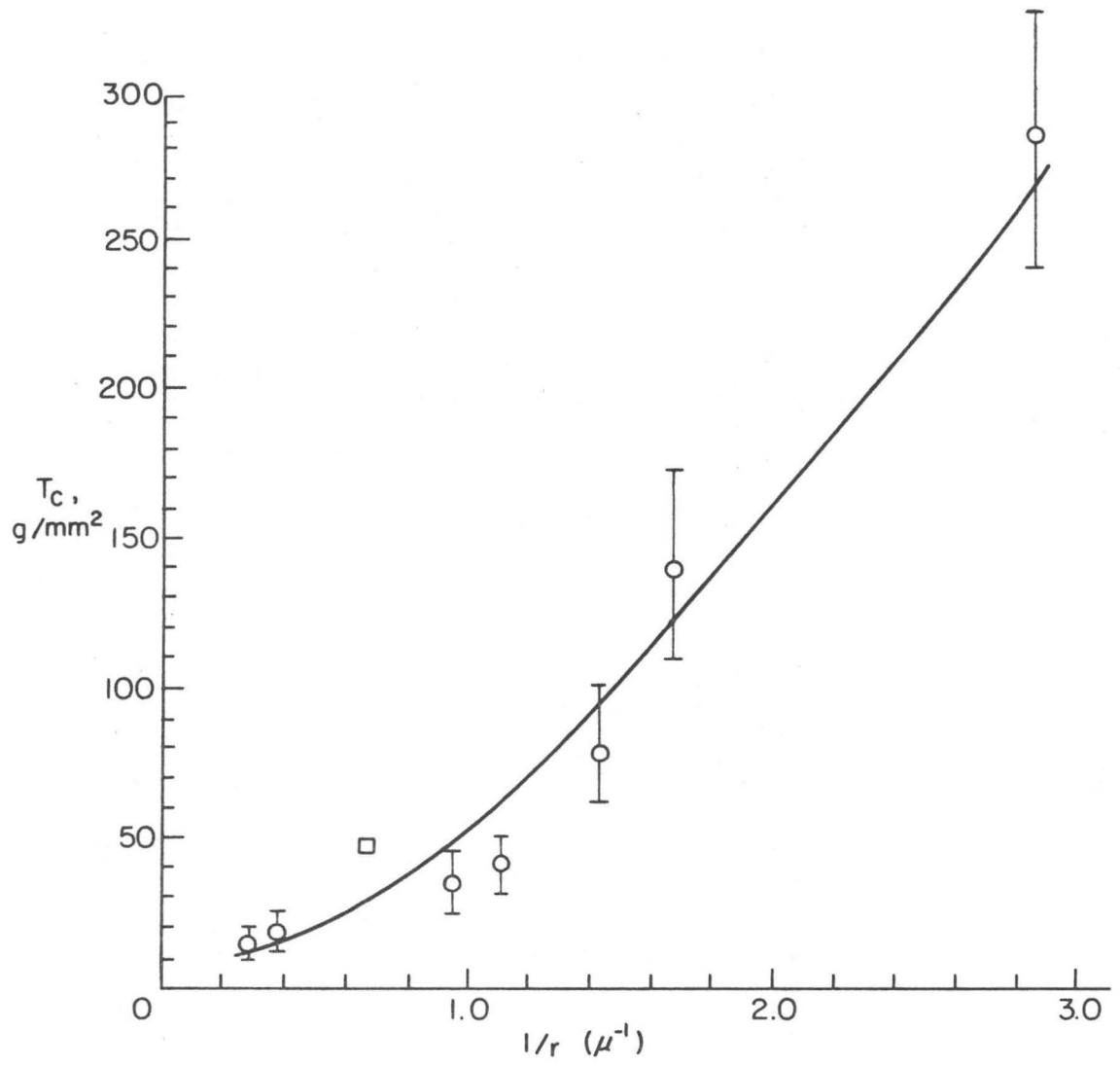
XBL 705-964

Figure 14a



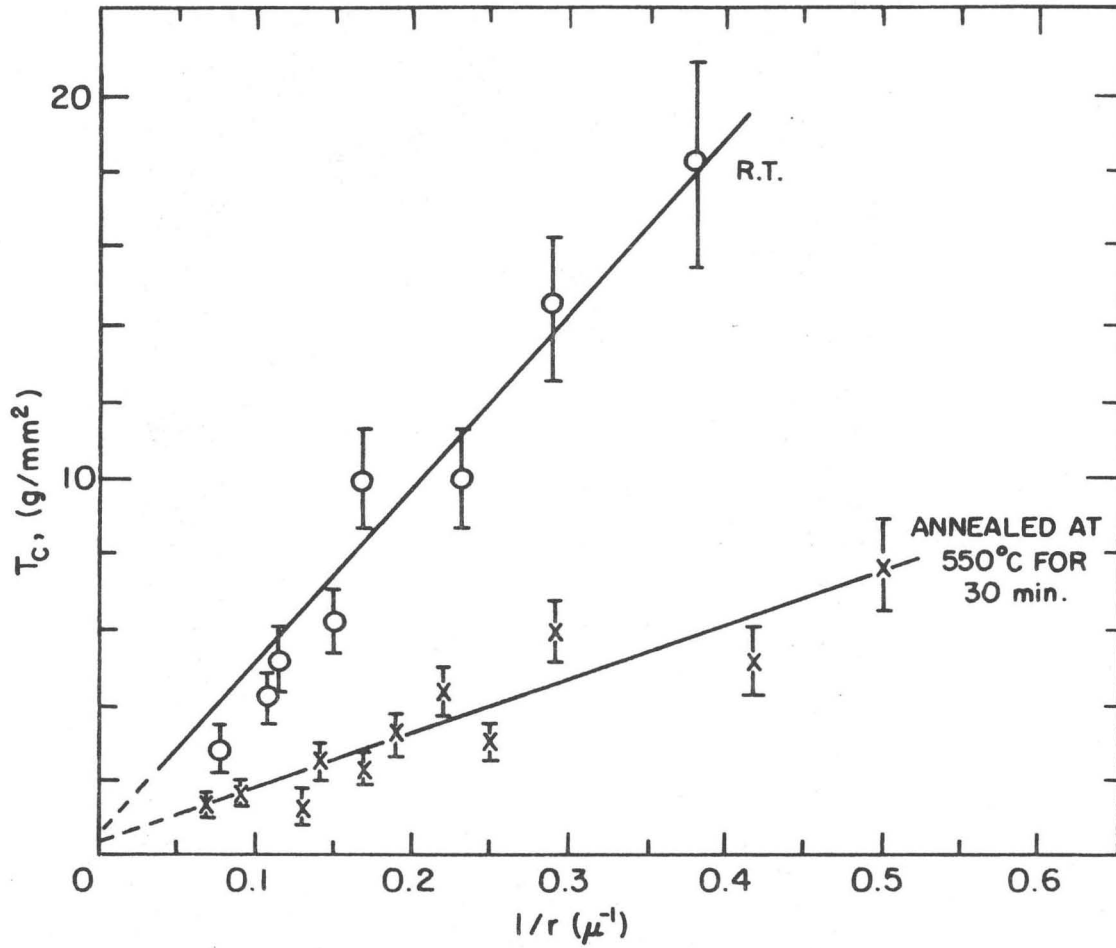
XBL 705-954

Figure 14b



XBL 705-955

Figure 15



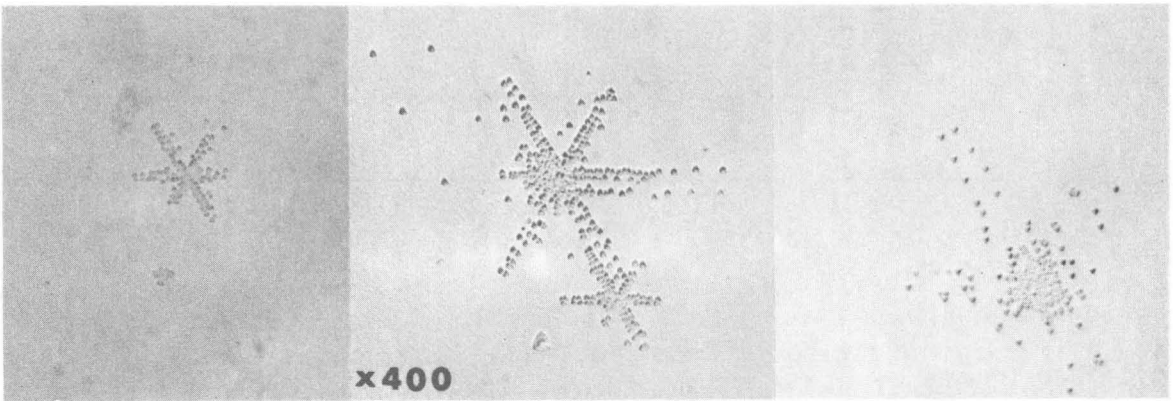
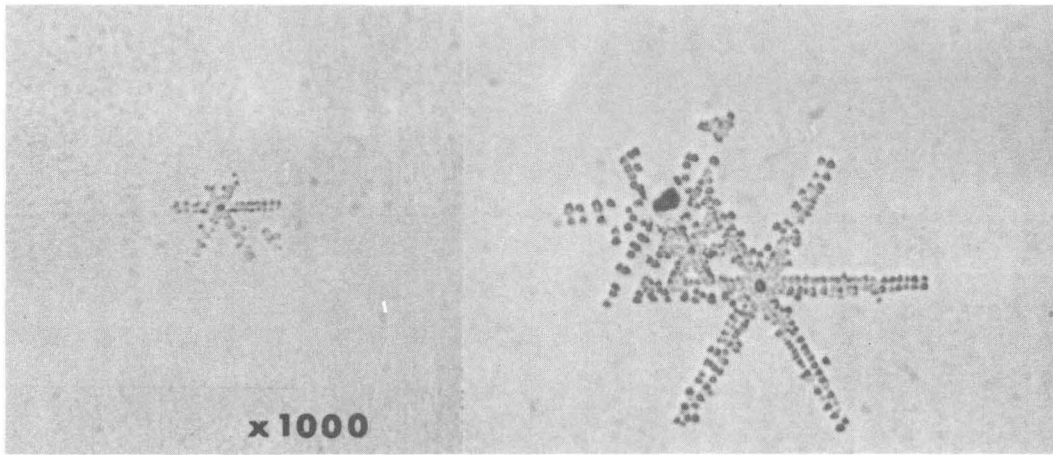
By the method of least squares

$$\text{R.T. } \tau_c = 49.1 (1/r) - 0.2$$

$$550^\circ\text{C } \tau_c = 14.1 (1/r) + 0.4$$

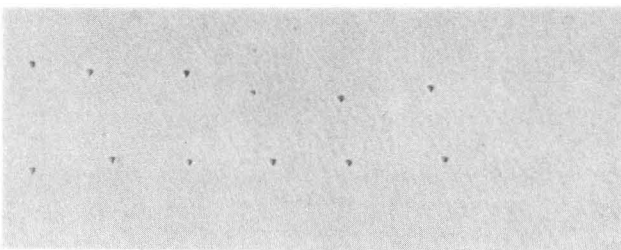
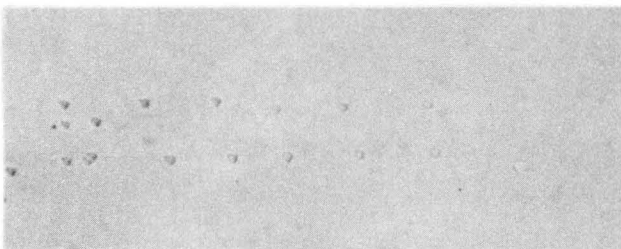
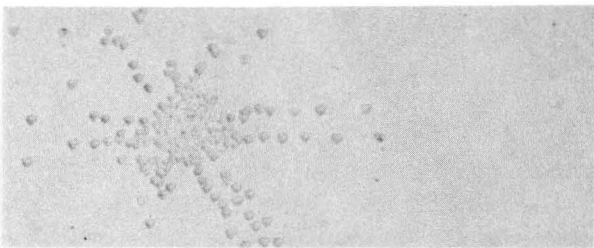
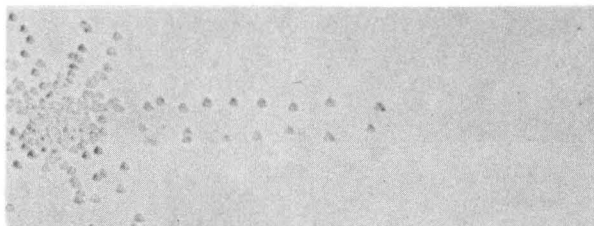
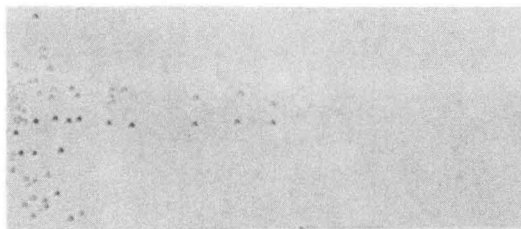
XBL 708-1676

Figure 16



XBB704-1997

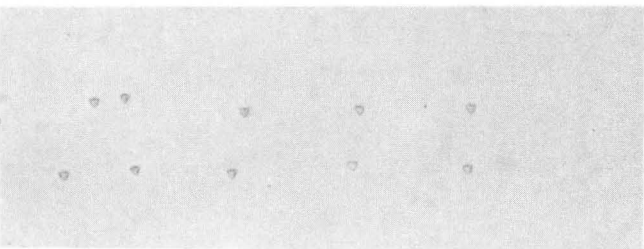
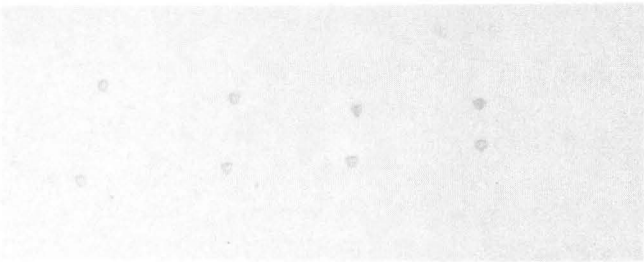
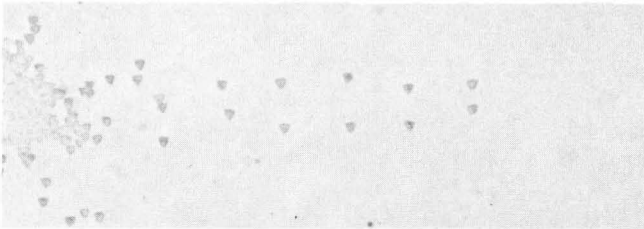
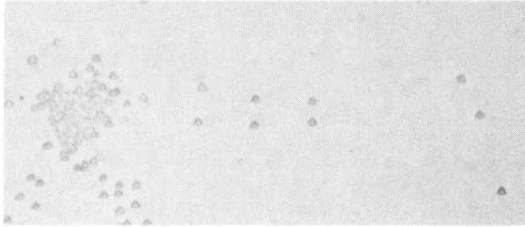
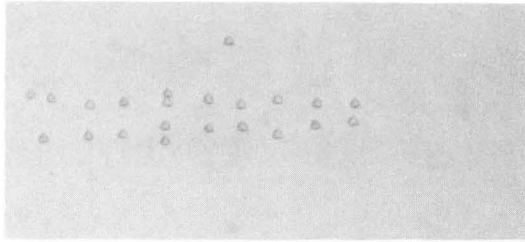
Figure 17a



XBB704-2004

x 400

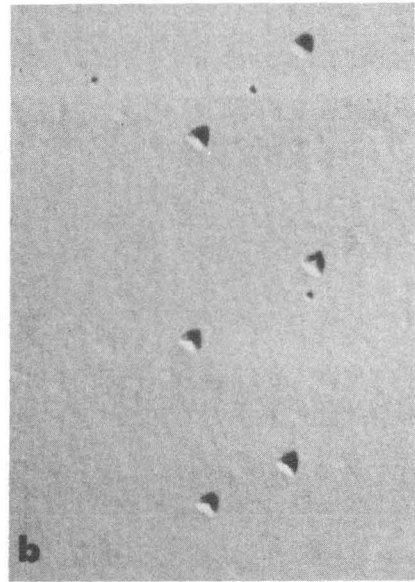
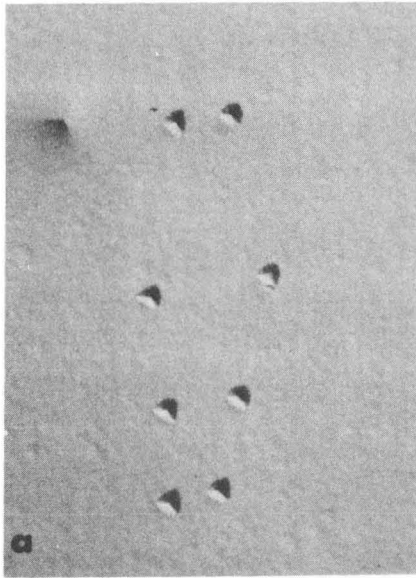
Figure 17a'




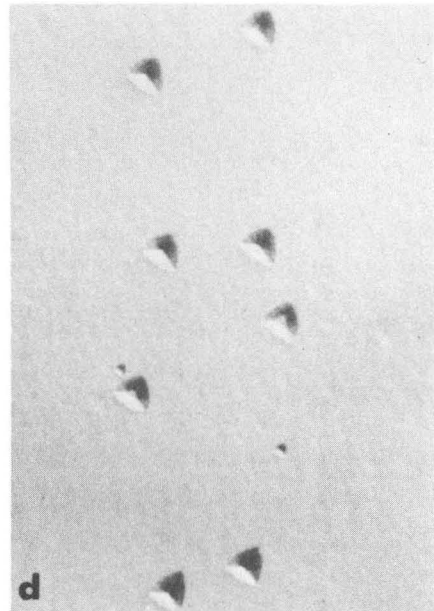
XBB704-2002

x 400

Figure 17b

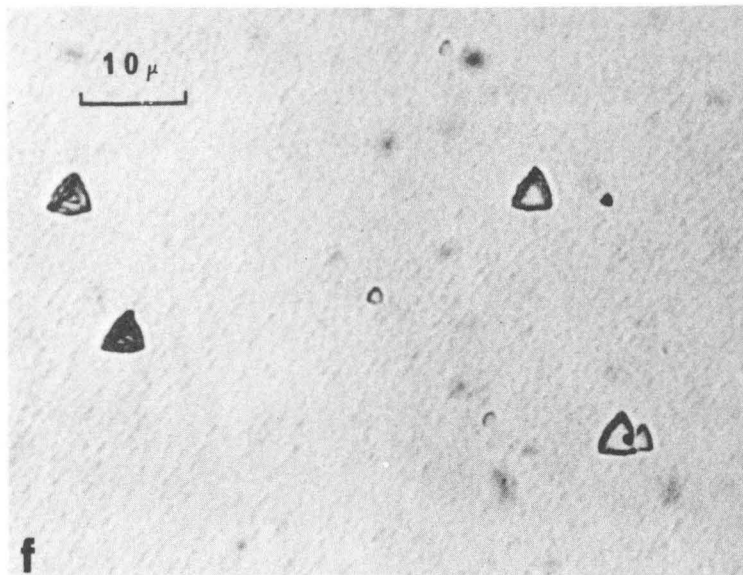
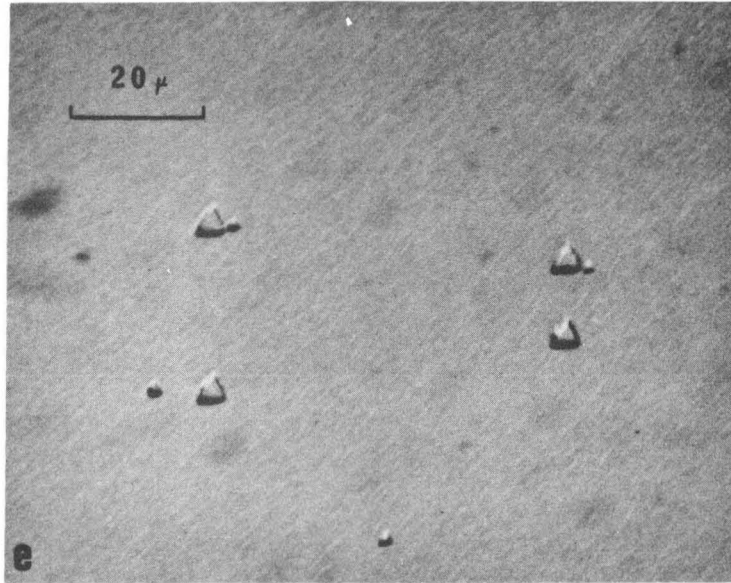


50 μ

A horizontal scale bar with a bracket underneath, indicating a length of 50 micrometers.

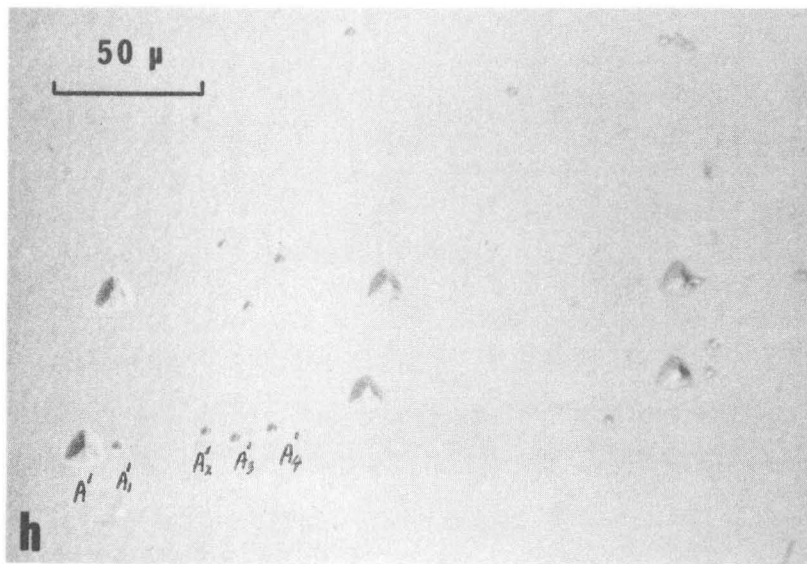
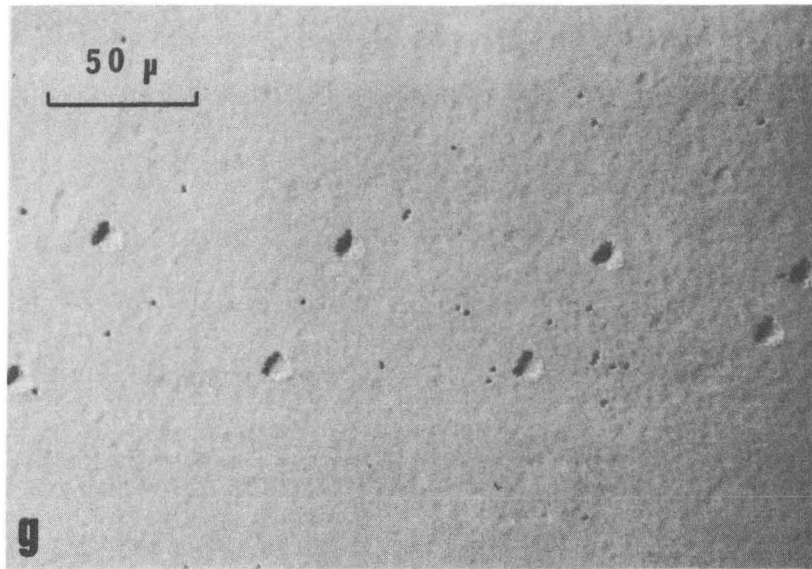
XBB704-2005

Figure 18



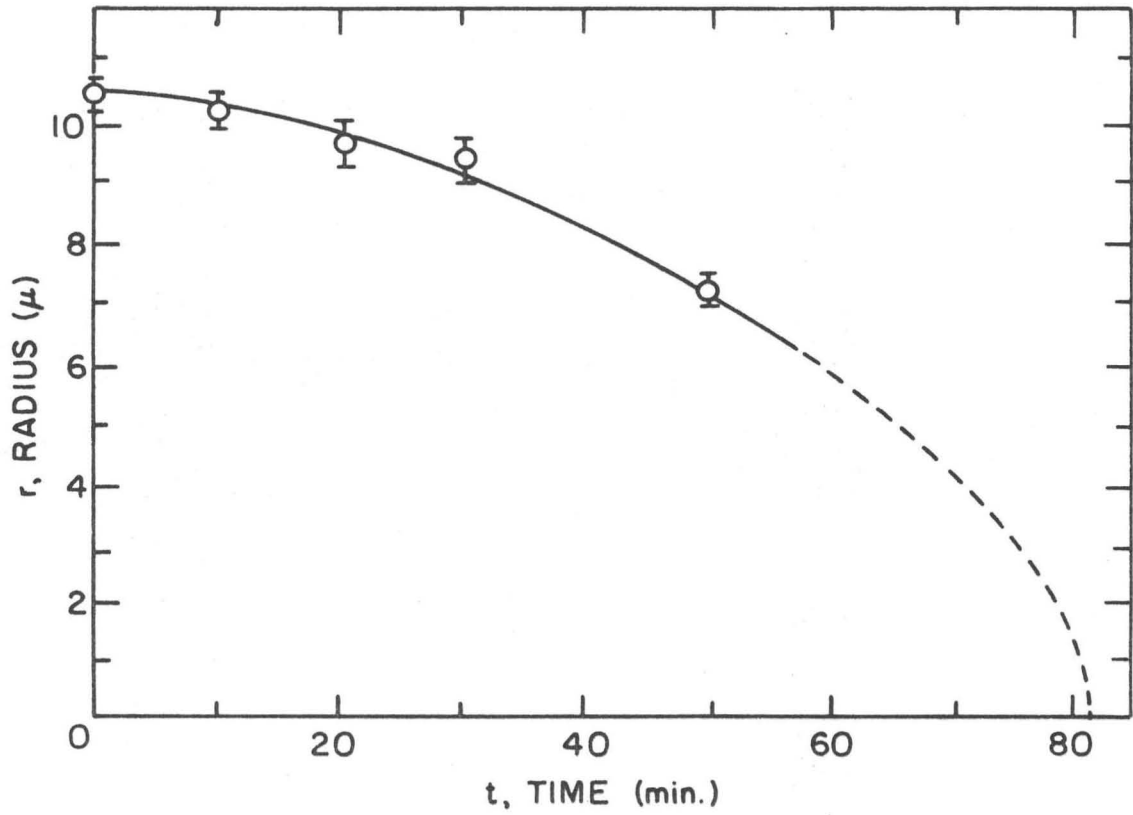
XBB704-1996

Figure 18 continued



XBB704-1998

Figure 18 continued

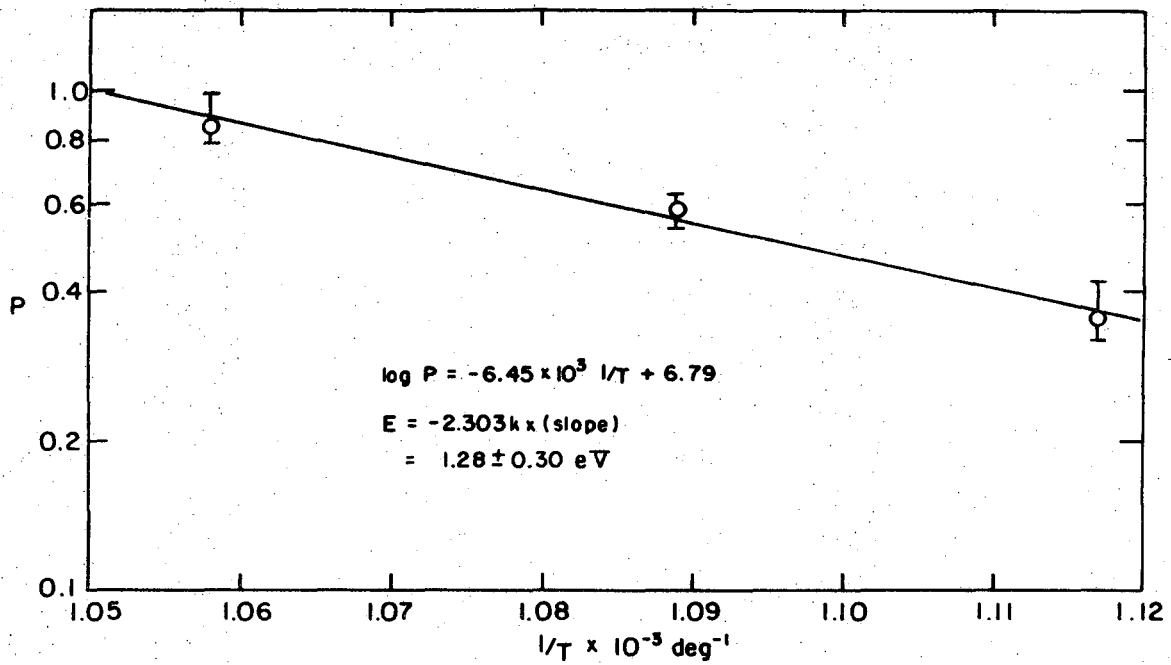


$$t - 82.7 = -0.68 r^2$$

(By the method of least squares)

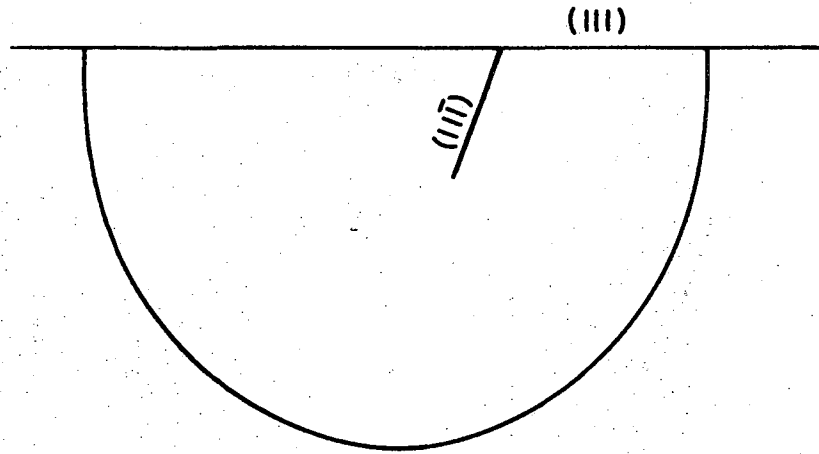
XBL 708-1675

Figure 19

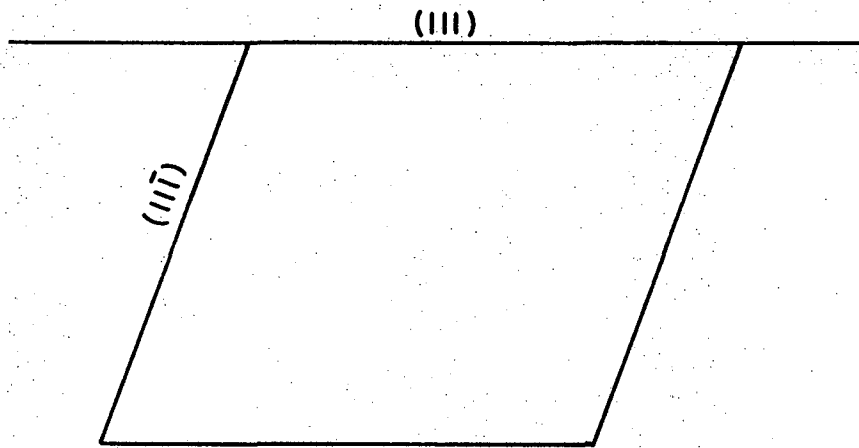


XBL 708-1677

Figure 20



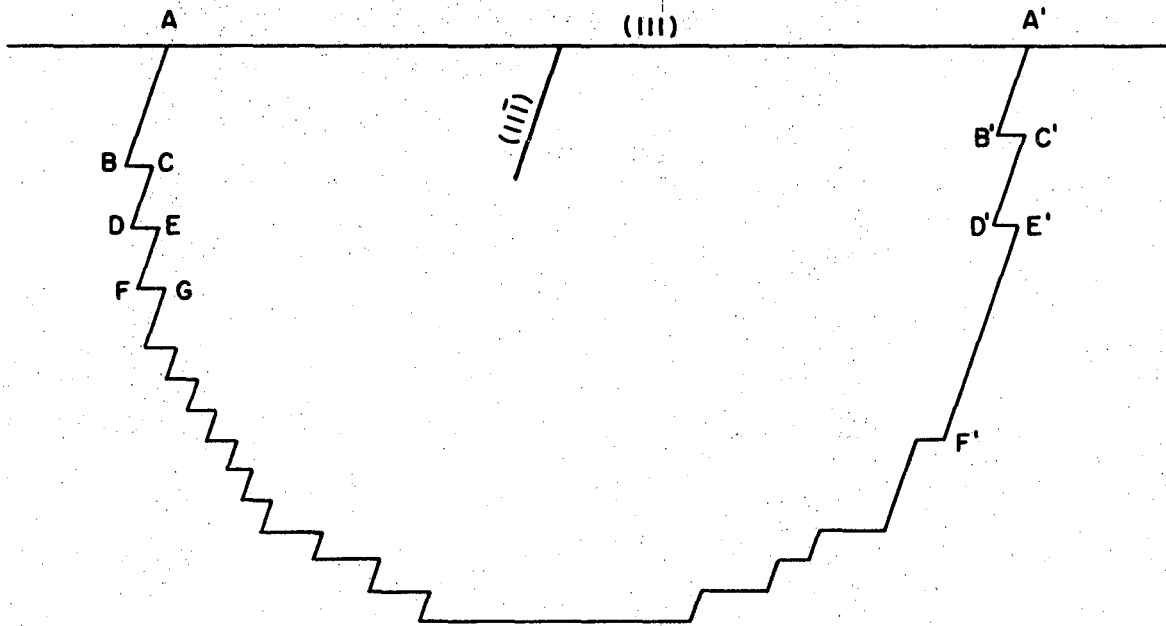
a.



b.

XBL 705-957

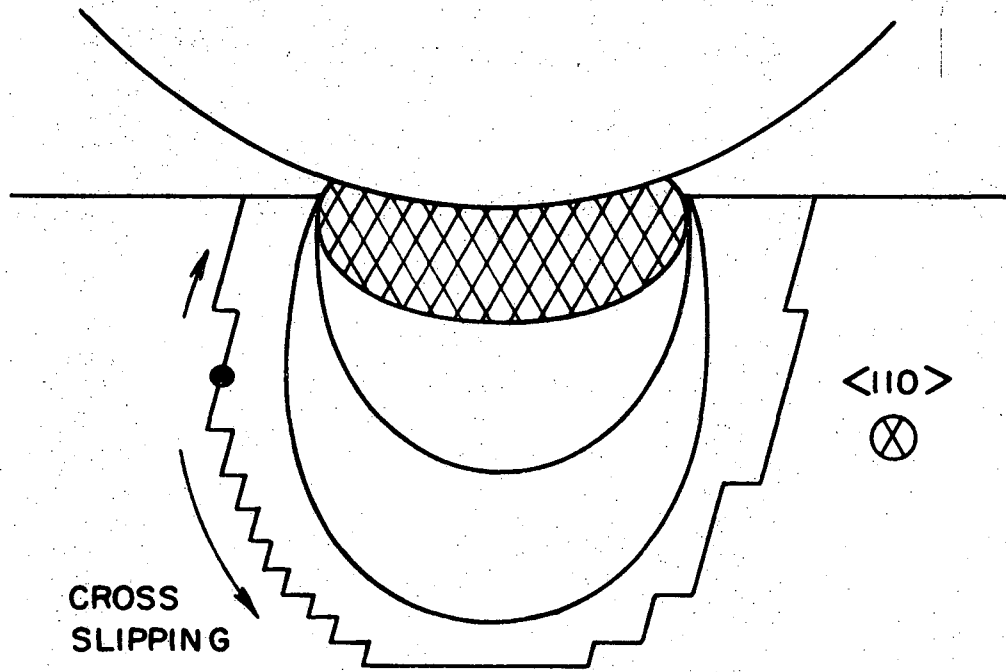
Figure 21



XBL 705-956

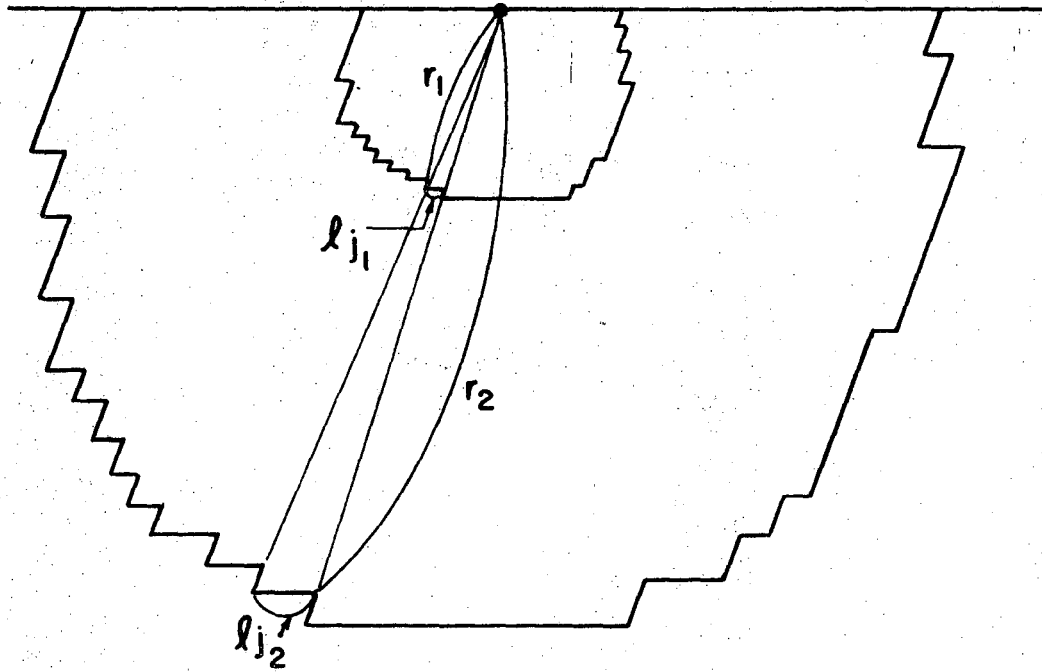
Figure 22

GLASS BALL



XBL 705-960

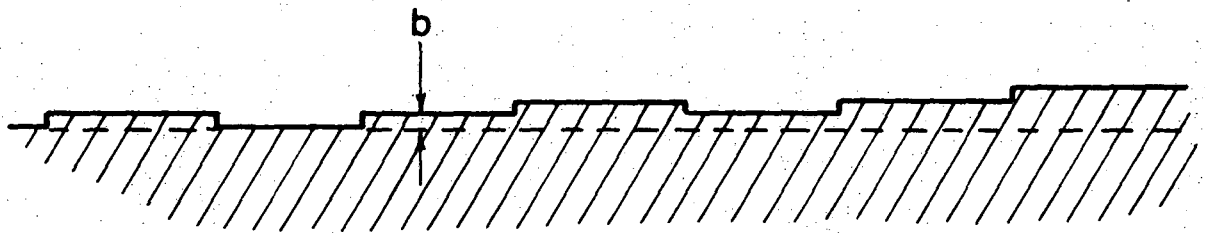
Figure 23



$$\frac{l_{j_1}}{l_{j_2}} = \frac{r_1}{r_2}$$

XBL 705-963

Figure 24



XBL 707-1371

Figure 25

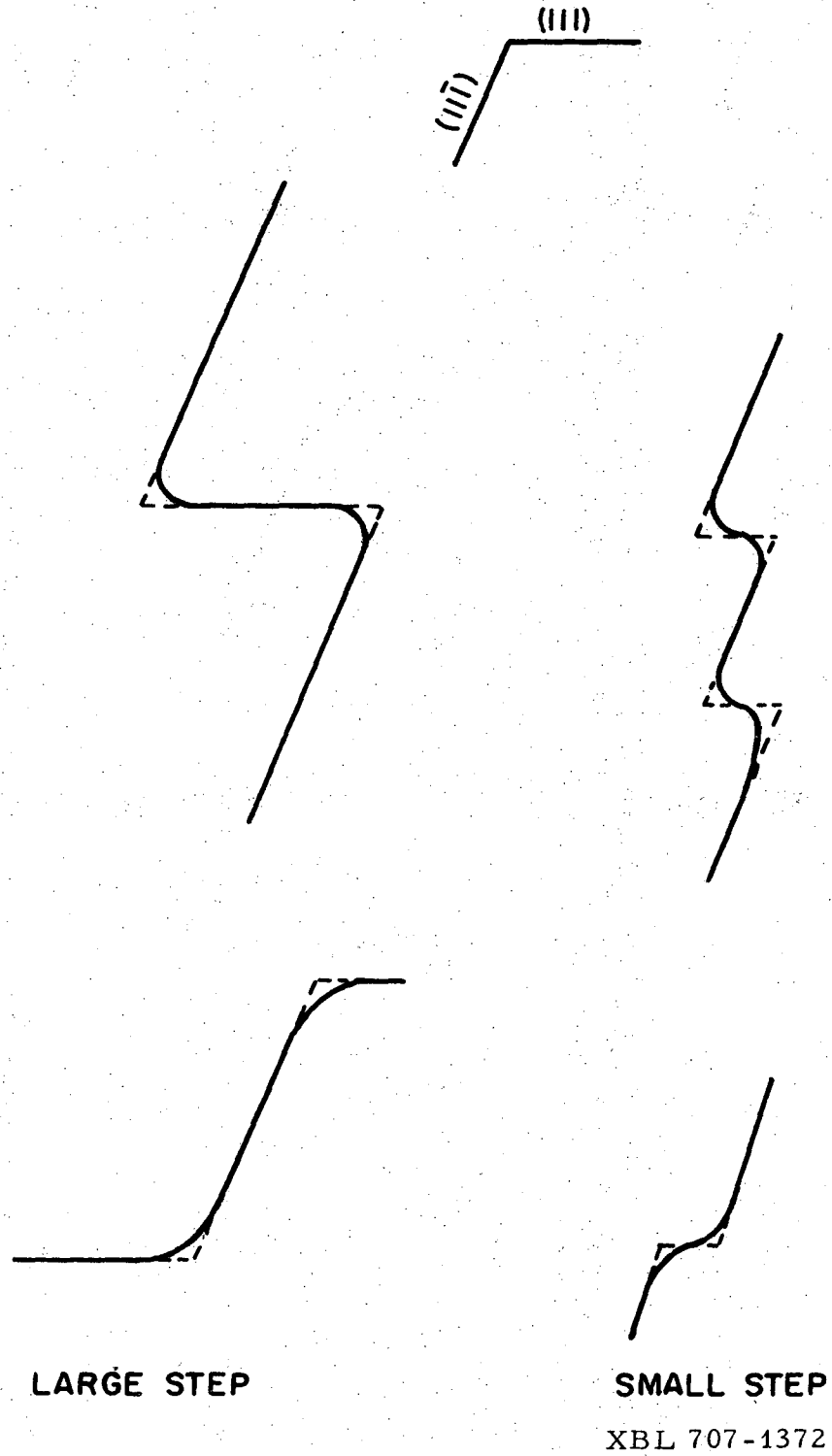
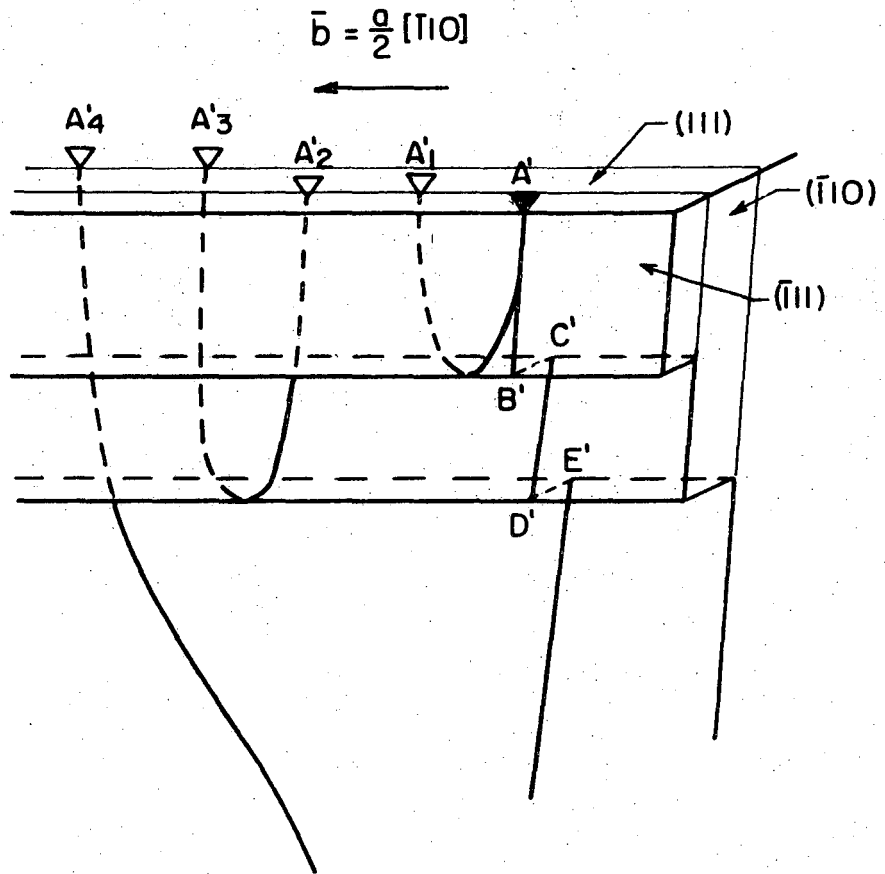
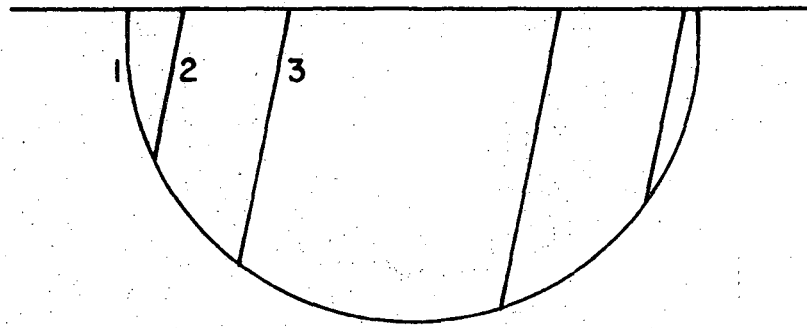


Figure 27

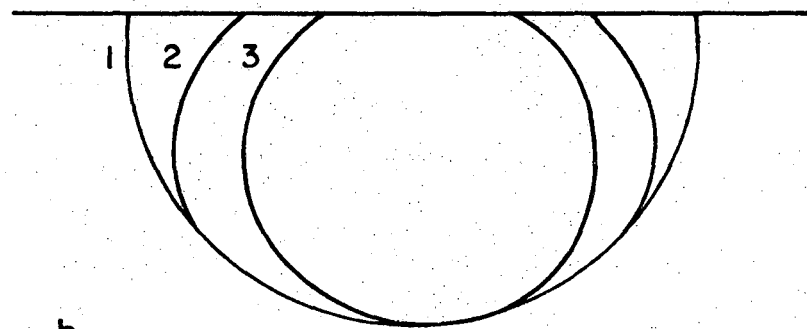


XBL 707-1368

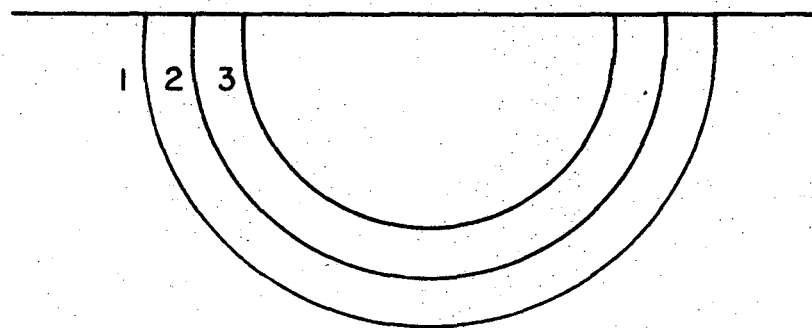
Figure 28



a.



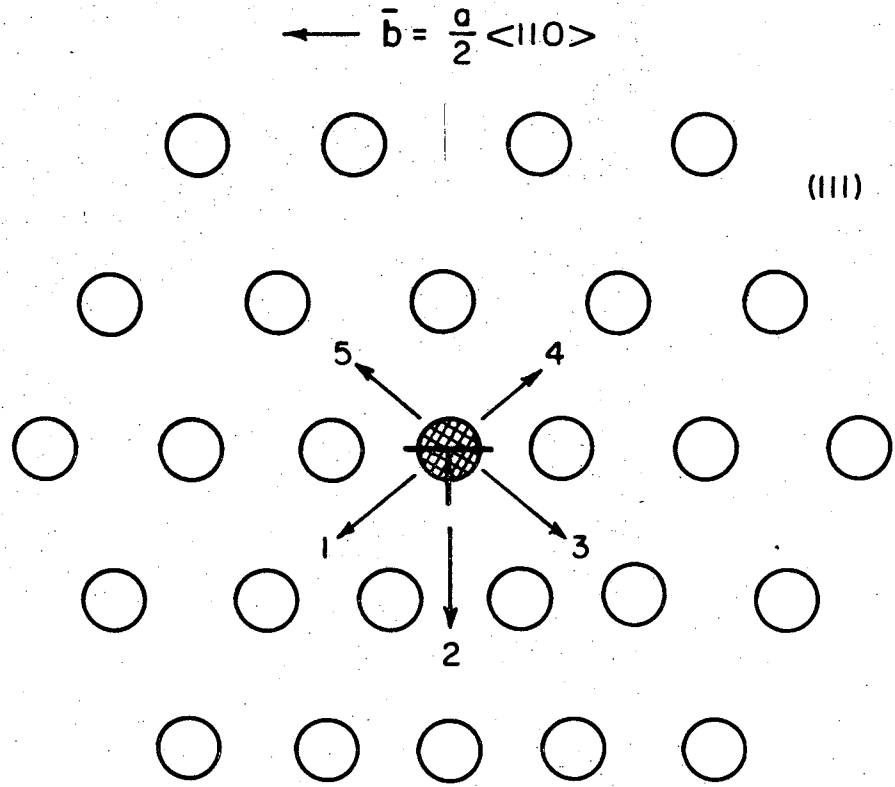
b.



c.

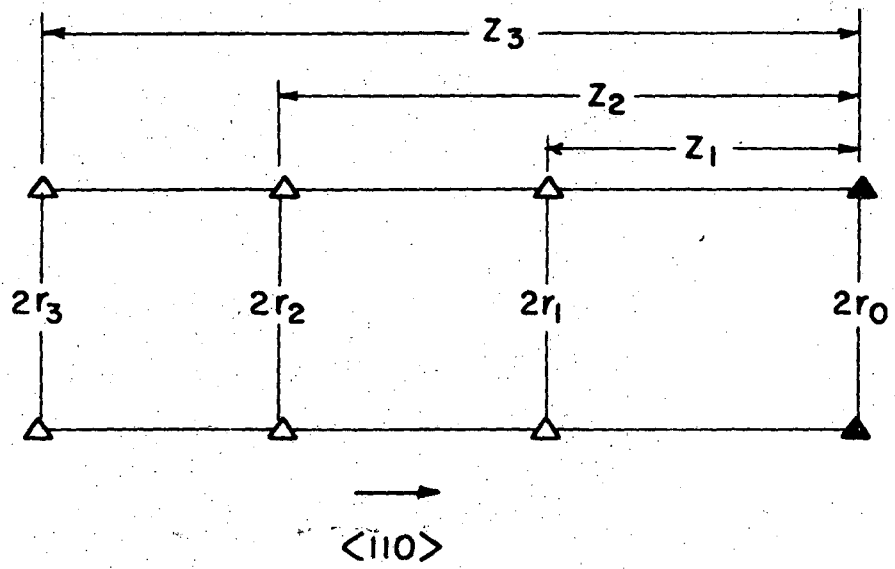
XBL 707-1373

Figure 29



XBL 707-1369

Figure 30



XBL 707-1370

Figure 31

LEGAL NOTICE

This report was prepared as an account of Government sponsored work. Neither the United States, nor the Commission, nor any person acting on behalf of the Commission:

- A. Makes any warranty or representation, expressed or implied, with respect to the accuracy, completeness, or usefulness of the information contained in this report, or that the use of any information, apparatus, method, or process disclosed in this report may not infringe privately owned rights; or*
- B. Assumes any liabilities with respect to the use of, or for damages resulting from the use of any information, apparatus, method, or process disclosed in this report.*

As used in the above, "person acting on behalf of the Commission" includes any employee or contractor of the Commission, or employee of such contractor, to the extent that such employee or contractor of the Commission, or employee of such contractor prepares, disseminates, or provides access to, any information pursuant to his employment or contract with the Commission, or his employment with such contractor.

TECHNICAL INFORMATION DIVISION
LAWRENCE RADIATION LABORATORY
UNIVERSITY OF CALIFORNIA
BERKELEY, CALIFORNIA 94720